

# Journal of Materials Chemistry A

Materials for energy and sustainability

Accepted Manuscript

This article can be cited before page numbers have been issued, to do this please use: M. Tsakanika, A. Stergiou, C. Pantazidis and G. Sakellariou, *J. Mater. Chem. A*, 2026, DOI: 10.1039/D6TA01035K.



This is an Accepted Manuscript, which has been through the Royal Society of Chemistry peer review process and has been accepted for publication.

Accepted Manuscripts are published online shortly after acceptance, before technical editing, formatting and proof reading. Using this free service, authors can make their results available to the community, in citable form, before we publish the edited article. We will replace this Accepted Manuscript with the edited and formatted Advance Article as soon as it is available.

You can find more information about Accepted Manuscripts in the [Information for Authors](#).

Please note that technical editing may introduce minor changes to the text and/or graphics, which may alter content. The journal's standard [Terms & Conditions](#) and the [Ethical guidelines](#) still apply. In no event shall the Royal Society of Chemistry be held responsible for any errors or omissions in this Accepted Manuscript or any consequences arising from the use of any information it contains.

# Single-ion Solid Polymer Electrolytes by Design: View Article Online DOI: 10.1039/D6TA01035K

## Chemistries, Architectures and Functional Trade-Offs

*Marileta Tsakanika, Anastasia Stergiou, Christos Pantazidis\*, Georgios Sakellariou\**

Laboratory of Industrial Chemistry, Department of Chemistry, National and Kapodistrian University of Athens, Panepistimiopolis, Zografou, 15771 Athens, Greece

**KEYWORDS.** Single-ion, Solid polymer electrolytes, Macromolecular architecture

### ABSTRACT

This review highlights recent advances in single-ion polymer electrolytes (SIPEs), with particular emphasis on how molecular design, through tailored chemistries, macromolecular architectures, and controlled morphologies, governs their structure–properties relationship. We examine emerging strategies that link ion transport, mechanical behavior, and electrochemical stability to specific molecular and supramolecular features, providing an overview of the most recent developments in the field. In parallel, a growing shift toward a holistic approach in material design is noted, where SIPEs are increasingly evaluated not only as fundamental ion-conducting systems but as multifunctional materials capable of integration into practical devices. By connecting molecular engineering with processing considerations and long-term functionality, this review outlines how SIPEs research is evolving toward materials-oriented solutions that support their translation into robust, high-performance technologies.



## 1. Introduction

View Article Online  
DOI: 10.1039/D6TA01035K

As global interest in cleaner energy systems continues to grow, technological innovation has become a central driver in shaping the future of power generation. Renewable-energy technologies such as solar, wind, and tidal power are advancing rapidly, increasing their accessibility and accelerating their deployment worldwide<sup>1</sup>. However, the variable nature of these resources introduces challenges for maintaining consistent and reliable electricity. Addressing these fluctuations requires equally rapid progress in energy-storage technologies. The need is particularly evident in the transportation sector, where the expanding adoption of electric vehicles demands lightweight, safe, and high-energy-density rechargeable batteries<sup>2</sup>. As more industries transition toward electrification, developing next-generation battery technologies has become essential for supporting a stable and adaptable energy landscape. Solid polymer electrolytes (SPEs), formed by dissolving lithium salts in polar polymer matrices without the use of volatile organic solvents, represent a promising pathway toward safer and more versatile batteries. Their resistance to leakage and flammability, coupled with the ability to tune mechanical, thermal, and ion-transport properties through polymer design, has positioned SPEs as strong candidates for future lithium-based electrochemical systems<sup>3-7</sup>. Within this class, single-ion polymer electrolytes (SIPEs) have emerged as particularly compelling<sup>8-10</sup>. Unlike conventional dual-ion polymer electrolytes, in which both cations and anions migrate during operation, SIPEs incorporate the counter anion directly into the polymer backbone. This structural tethering immobilizes the anion, leaving lithium ions as the sole mobile charge carriers, which provides significant improvements. The ideal lithium-ion transference number,  $t_{\text{Li}^+}$ , approaches unity in SIPEs, whereas in dual-ion systems it typically remains near  $\sim 0.2$ . In such dual-ion systems, preferential solvation of  $\text{Li}^+$  creates a relatively bulky coordination shell that diffuses more slowly than the free counter anion<sup>11,12</sup>. This imbalance results in substantial anion mobility and, consequently, pronounced concentration polarization at the electrodes. Such polarization increases cell resistance, shortens cycle life, and accelerates dendritic lithium growth, one of the primary failure mechanisms in lithium-metal batteries. By suppressing anion mobility, SIPEs offer a route to mitigate these limitations and enable more stable, high-performance operation<sup>13,14</sup>. Despite significant progress, several key challenges continue to limit the practical implementation of SIPEs. These include the intrinsic trade-off between ionic conductivity and mechanical robustness, limited interfacial stability with lithium metal and high-voltage cathodes, and difficulties in achieving processability and scalability without compromising performance. In addition, the strong coupling between ion transport and polymer segmental



dynamics, as well as the complex interplay between anion chemistry, polymer polarity and morphology, complicates the rational design of high-performance systems. In this context, a comprehensive framework that connects molecular design to macroscopic properties is needed. To address these challenges, growing interest in SIPEs has driven rapid development of molecular, structural, and materials-based design strategies aimed at optimizing performance. In this review, we organize recent advances by molecular architecture, distinguishing between linear and non-linear polymer systems (Figure 1). For linear SIPEs, we focus on how chemical structure governs key material properties, including ion-pair dissociation, counter anion identity and stability, polymer polarity and miscibility, segmental mobility, and crystallization behavior. In contrast, non-linear architectures, such as grafts, stars, nanoparticles, and networks, are often designed to manipulate morphology, mechanical robustness, processability, or the decoupling of ion transport from segmental dynamics. These more complex systems are therefore categorized according to their design rationale and the functional objectives they aim to address.

Growing interest in SIPEs has driven rapid development of molecular, structural, and materials-based design strategies aimed at optimizing performance. In this review, we organize recent advances by molecular architecture, distinguishing between linear and non-linear polymer systems (Figure 1). For linear SIPEs, we focus on how chemical structure governs key material properties, including ion-pair dissociation, counter anion identity and stability, polymer polarity and miscibility, segmental mobility, and crystallization behavior. In contrast, non-linear architectures, such as grafts, stars, nanoparticles and networks, are often designed to manipulate morphology, mechanical robustness, processability, or the decoupling of ion transport from segmental dynamics. These more complex systems are therefore categorized according to their design rationale and the functional objectives they aim to address.

View Article Online  
DOI: 10.1039/D6TA01035K



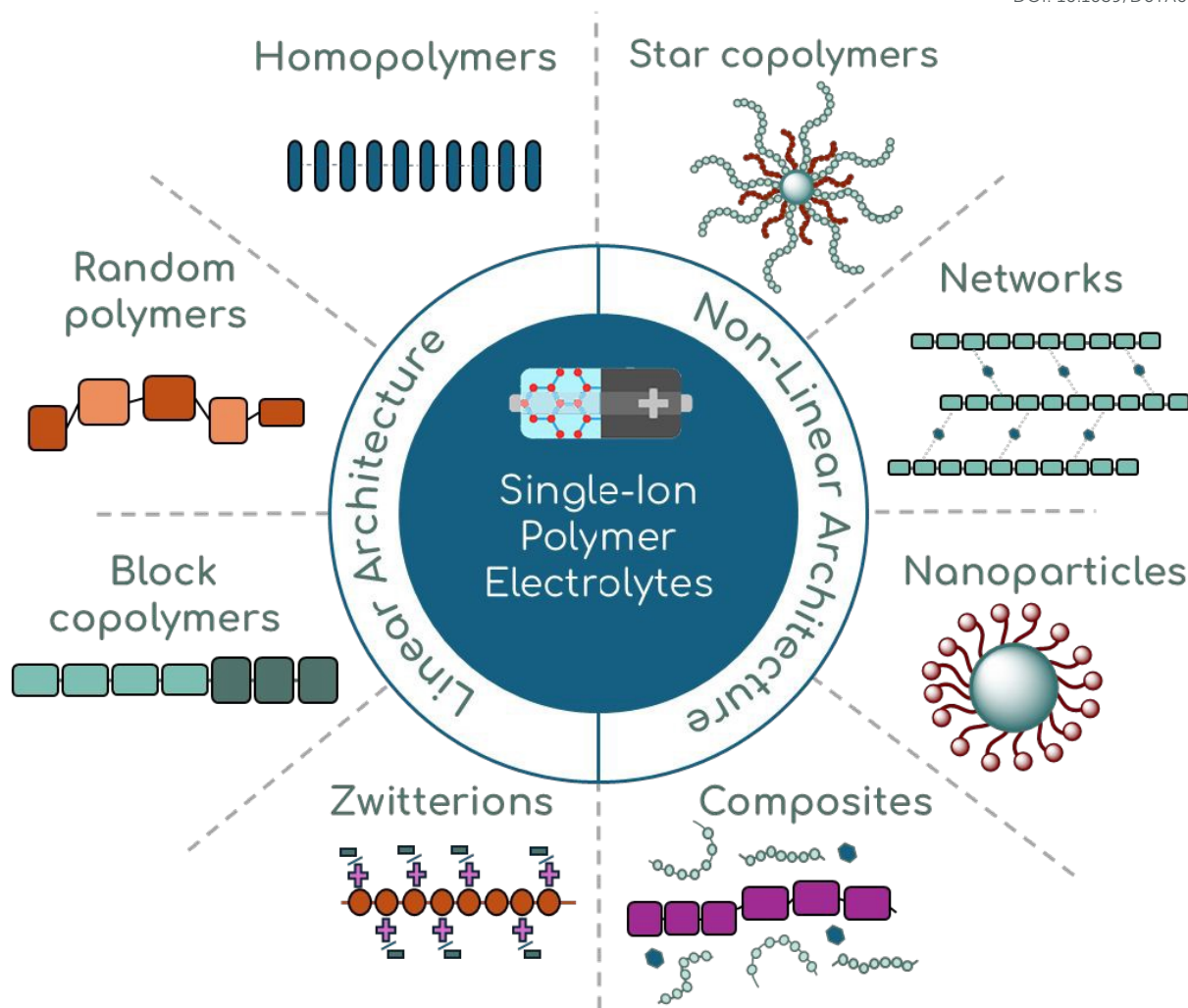


**Figure 1.** Schematic representation of recent developments in single-ion polymer electrolytes (SIPEs), organized by molecular architecture into linear and non-linear polymer systems.



## 2. Linear Polymer Systems: Structure-Properties Relationship in SIPEs

View Article Online  
DOI: 10.1039/D6TA01035K

The following section classifies linear single-ion polymer electrolytes according to their underlying chemical frameworks, reflecting how backbone composition and functional group chemistry dictate ion transport and mechanical behavior. In these systems, Li<sup>+</sup> transport generally proceeds through coordination with polar sites on the polymer chains and migration assisted by local segmental motion, making ion mobility closely coupled to polymer dynamics and the flexibility of the amorphous phase<sup>6,10,15,16</sup>. By examining distinct polymer families, the discussion highlights how variations in molecular structure, such as backbone rigidity, polarity, and the nature of the tethered anion, govern key structure–property relationships. This chemistry-based organization provides a foundation for understanding how targeted molecular design can balance conductivity, stability, and mechanical performance in linear SIPE systems.

### 2.1 Polystyrene-based SIPEs

A widely used strategy to enhance lithium transport in single-ion polymer electrolytes, is to replace semicrystalline poly(ethylene oxide) (PEO) with fully amorphous analogs, thereby improving segmental mobility. Ghorbanzade et al<sup>17</sup>. implemented this approach by substituting PEO with poly(propylene oxide) (PPO), which remains amorphous due to its pendant methyl groups. When blended with PPO segments and combined with a plasticizer and low levels of lithium salt dopant, without forming a conventional salt-in-polymer system (Figure 2a), the polystyrene-based single-ion polymer electrolyte (PSTFSILi) demonstrated nearly twice the ionic conductivity compared to the pristine material. However, at higher salt loadings, mechanical instability and phase separation emerged, highlighting the delicate balance between conductivity enhancement and morphological stability. Building on this theme of facilitating ion motion, Kondou et al.<sup>18</sup> investigated solvent-assisted transport using lithium poly(styrenesulfonyl(trifluoromethanesulfonyl)amide) (PSTFSLi) in ethylene carbonate/dimethyl carbonate (EC/DMC) mixtures (Figure 2b), to facilitate ion motion. In low-polarity blends, conductivities exceeding 1 mS cm<sup>-1</sup> (at 30 °C) were observed at high salt concentrations, with low activation energy indicating efficient ion hopping. Notably, full-cell tests with LiFePO<sub>4</sub> cathodes demonstrated stable cycling and excellent rate capability, attributed to reduced interfacial resistance within the optimized solvent environment.

While solvent-based approaches can enhance ion mobility, more durable improvements have arisen from tailoring polymer structure. Zhao et al.<sup>19</sup> systematically investigated copolymers of STFSILi with comonomers ranging from flexible, nonpolar units to polar, high-dielectric groups (Figure 2c). Precise compositional control was achieved through RAFT polymerization,



revealing that nonpolar segments led to poor miscibility and low conductivity, whereas strongly polar groups increased the glass transition temperature and restricted chain motion. The study concluded that effective SIPEs require not only appropriate polarity but also charge delocalization and strong miscibility between conducting and plasticizing domains to maintain a low  $T_g$  and promote efficient ion transport. Another strategy was demonstrated by Shao et al.<sup>20</sup>, who developed styrene-based BAB-type triblock copolymers incorporating PEO segments within the backbone (Figure 2d). Using PEO as a macroinitiator followed by ATRP of lithium (N-tetrafluorophenyl)trifluoromethanesulfonamide (TfnPFS), precise control was achieved over the ionic content. Notably, excessive ionic loading ( $[EO]:[Li] = 88$ ) diminished conductivity due to aggregation, whereas an intermediate composition ( $[EO]:[Li] = 40$ ) exhibited enhanced conductivity, particularly at elevated temperatures where PEO became fully amorphous ( $5.7 \cdot 10^{-6}$  and  $9.7 \cdot 10^{-6}$  S  $cm^{-1}$  at 70 and 90 °C, respectively).

Attention has also turned to anion design, aiming to reduce fluorine content while enhancing electrochemical stability. Yuan et al.<sup>21</sup> introduced a cyano-substituted, charge-delocalized anion (PCSiLi) that improved stability and mitigated environmental concerns associated with fluorinated sulfonyl groups (Figure 2e). When blended with PEO, the resulting electrolyte exhibited mechanical flexibility, high thermal stability ( $>300$  °C), and a low glass transition temperature, achieving a lithium-ion transference number of 0.84 and an extended electrochemical window up to 5.5 V. Long-term cycling was maintained for hundreds of hours without short-circuiting, and full cells demonstrated stable capacity retention. Advancing charge delocalization further, Martinez-Ibañez et al.<sup>22</sup> developed a fluorine-free, dicyano-substituted polyanion, lithium poly(4-styrenesulfonyl)(dicyano)methide (PSDMLi) (Figure 2f). This polyelectrolyte, synthesized via free-radical polymerization, achieved a lithium transference number as high as 0.95 while retaining good thermal stability. Computational analysis corroborated the experimental findings by showing that all fluorine-free systems exhibit lower  $Li^+$  dissociation energies compared to conventional fluorinated analogues. While this confirms that charge delocalization contributes to ion mobility, the results also highlight that anion flexibility and polymer segmental motion are decisive factors governing the overall ionic conductivity.



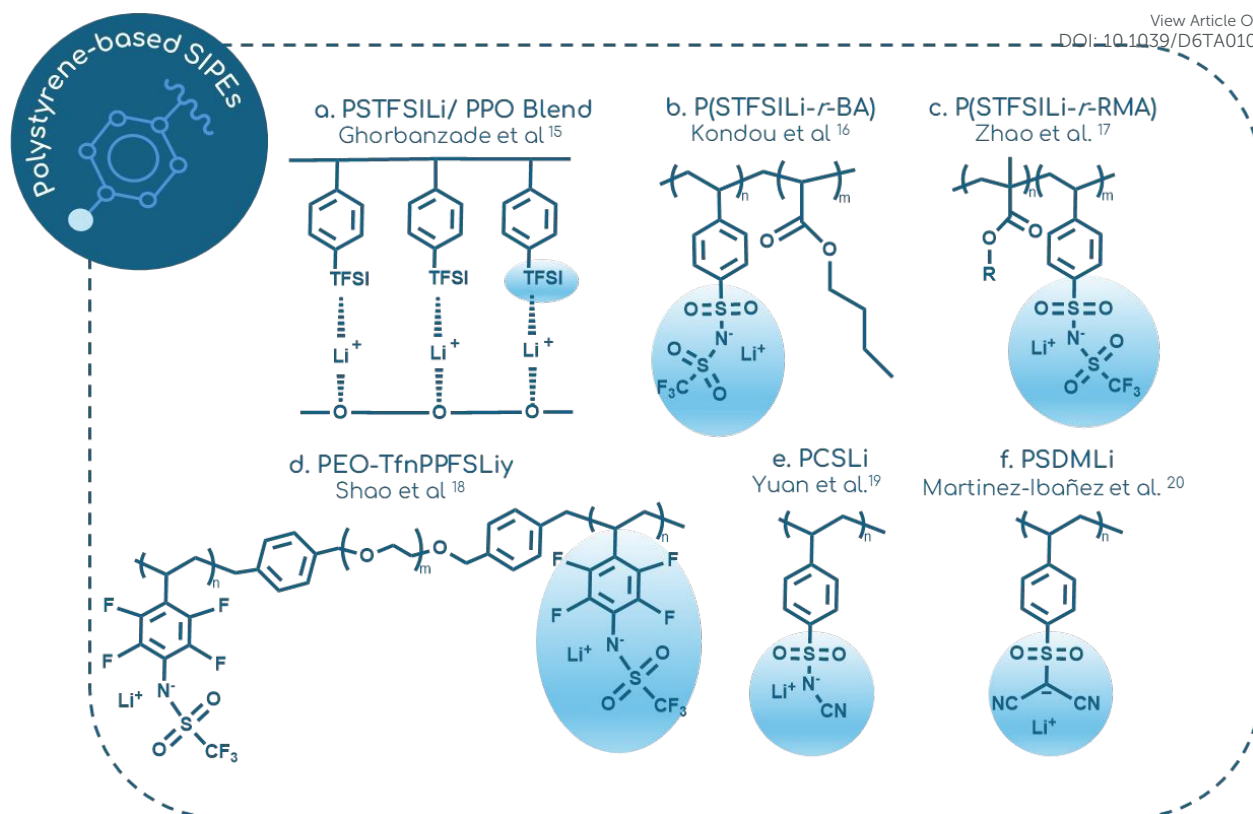


**Figure 2.** Overview of the chemical structures of polystyrene-based single-ion polymer electrolytes discussed in Section 2.1. The highlighted regions indicate the pendant ion-bearing groups, emphasizing the structural variations in the ionic moieties attached to the polymer framework.

Overall, polystyrene-based SIPEs show that conductivity can be improved through multiple, partially complementary levers: suppressing crystallinity, increasing segmental mobility, promoting charge delocalization, and optimizing miscibility between conducting and plasticizing domains. Across these studies, the most effective systems are not simply the most polar or the most highly functionalized, but those in which anion chemistry and local chain dynamics are tuned together. Fluorine-free charge-delocalized anions emerge as particularly promising because they can preserve high  $t_{\text{Li}^+}$  and electrochemical stability while reducing environmental concerns, although conductivity still remains strongly dependent on backbone flexibility. Thus, for this family, the key structure–property lesson is that ion dissociation alone is insufficient unless accompanied by adequate segmental motion and morphological stability.

## 2.2 Polymethacrylate-based SIPEs

Liu and Schaefer et al.<sup>23</sup> investigated the impact of tethering TFSI anions to various polymer backbones through a 10-methylene spacer to intentionally promote ion aggregation (Figure 3a). Polystyrene copolymers self-assembled into lamellar ionic domains via phase separation, whereas acrylate and methacrylate counterparts formed only disordered clusters. Consequently,



methacrylate-based SIPEs, despite their chemical versatility, exhibited the lowest conductivity due to strong lithium-backbone interactions. Dielectric analysis revealed that ion transport was governed more by the organization and relaxation of ionic groups than by the overall backbone mobility, underscoring the crucial influence of local polarity and rigidity.

To highlight the critical role of anion chemistry, Mei et al.<sup>24</sup> compared sulfonylimide and sulfonate lithium methacrylate comonomers in PEG methacrylate copolymers synthesized via RAFT polymerization (Figure 3b). Sulfonylimide copolymers exhibited significantly higher conductivity and diffusivity, despite their higher glass transition temperatures, owing to charge delocalization that mitigated ion aggregation. In contrast, sulfonate analogues benefited from lower  $T_g$  but suffered from stronger ion pairing. These trade-offs demonstrate that segmental mobility alone is insufficient without careful anion design to balance conductivity and thermal properties. The interplay between ionic content and morphology was further elucidated by Kadulkar et al.<sup>25</sup>, who synthesized solvent-free SIPEs through copolymerization of poly(ethylene glycol) methyl ether acrylate (PEGMEA) with various lithiated anions (Figure 3c). Adjusting the ratio of ionic groups to PEG side chains generated distinct transport regimes: at low ionic concentrations, lithium ions migrated via vehicular co-diffusion with the polyanion, whereas higher loadings facilitated ion hopping through interconnected aggregates. Morphology remained a key determinant; acrylic acetate (AA) copolymers exhibited phase-separated domains, while methacrylate-propyl (trifluoromethanesulfonyl) imide (MPTFSI) and 2-acrylamido-2-methylpropanesulfonate (AMPS) systems maintained more uniform dispersion. Nonetheless, ion transport remained strongly coupled to polymer segmental dynamics.

In an effort to decouple ion transport from polymer dynamics, Yang and Epps et al.<sup>26</sup> blended rigid PMTFSILi with flexible poly(oligo-oxyethylene) methyl ether methacrylate (POEM) to engineer a system that balances structural rigidity and chain mobility (Figure 3d). This approach traded morphological simplicity for enhanced performance: the rigid component introduced packing frustration, creating additional free volume for ion hopping, while the flexible POEM preserved segmental motion. The resulting materials exhibited high ionic conductivity ( $\sim 10^{-2}$  S  $\text{cm}^{-1}$  at 150 °C), a lithium-ion transference number of  $\sim 0.9$ , and broad electrochemical stability. However, the effectiveness of this strategy depended on careful compositional tuning, excessive rigidity reduced processability, whereas excessive flexibility diminished free volume. The blend approach thus provided a controlled means of decoupling ion transport from segmental dynamics.

Building on principles of controlled self-assembly, Chouirfa et al.<sup>27</sup> employed polymerization-induced self-assembly (PISA) to synthesize nanostructured block copolymers comprising



PEGMA and MASTFSILi segments, followed by a polystyrene block (Figure 3e). The resulting spherical aggregates were tunable via the length of the polystyrene block, and AFM characterization revealed short-range nanodomains (approximately 44 nm) within the hydrophilic regions. However, these disordered nanostructures alone did not support efficient ion transport; well-defined nanochannels formed only when the materials were blended with preassembled triblock copolymers. This work demonstrated that precise self-assembly can create ion-conducting pathways unattainable in random copolymers, emphasizing morphology as a design opportunity. Lozinskaya et al.<sup>28</sup> highlighted the interconnected roles of morphology and mechanical integrity using triblock copolymers composed of conductive lithiated methacrylate, polar (ethylene glycol)methyl ether methacrylate (PEGM), and rigid 2-phenylethyl methacrylate (PhEtM) segments (Figure 3f). With increasing molecular weight, the morphology transitioned from cylindrical to lamellar structures, the latter providing simultaneous improvements in ionic conductivity and mechanical robustness. The best-performance material achieved a conductivity of  $3.8 \times 10^{-7}$  S cm<sup>-1</sup> at 25 °C and a lithium-ion transference number of ~0.96 at 70 °C, while maintaining high storage modulus. In contrast to random copolymer systems, synthesized in the same study, these ordered lamellar domains supported stable cycling in Li-metal cells, although the overall conductivity remained moderate, relative to more flexible systems. Zhang et al.<sup>29</sup> investigated symmetric diblock copolymers composed of poly(OEGMA) and poly(OEG-propyl sodium sulfonate methacrylate) (Figure 3g), systematically varying the ionic content to examine its effect on morphology. Small-angle X-ray scattering (SAXS) revealed a sequence of structural transitions, from spherical to cylindrical to lamellar domains, as ionic content increased, each transition enhancing the connectivity of ion-conducting channels. Thus, it was demonstrated that increasing charge density and precisely tuning block ratios can promote the formation of continuous transport pathways, underscoring the critical influence of molecular architecture at ion conduction. Further advancing block copolymer design, Lozinskaya et al.<sup>30</sup> synthesized diblock systems comprising of rigid 2-phenylethyl methacrylate (PEM) segment and an ionic block of lithium methacrylate–sulfonimide (LiM/ MASTFSILi) statistically copolymerized with (ethylene glycol) methacrylate (PEGM) (Figure 3h). Incorporating as little as ~7 mol% MASTFSILi induced lamellar self-assembly with an interlayer spacing of approximately 28 nm. Although the ionic conductivity was modest ( $\sim 10^{-7}$  S cm<sup>-1</sup> at room temperature), it was tunable over four orders of magnitude through variation of the block ratio and MASTFSILi content reaching  $4.2 \times 10^{-7}$  S cm<sup>-1</sup> at 25 °C.



Complementary strategies have also emerged through blending and additive optimization. Wen et al.<sup>31</sup> combined lithiated methacrylate sulfonylimide with vinyl ethylene carbonate (VEC), incorporating poly(vinylidene fluoride) (PVDF) to enhance mechanical strength and succinonitrile as a plasticizer. This formulation achieved a balanced performance, with conductivity of around  $10^{-4}$  S cm<sup>-1</sup> at room temperature, electrochemical stability exceeding 4.5 V, and a high lithium-ion transference number of 0.93. Functional groups such as carbonyl and cyano-moieties coordinated lithium ions, supporting stable cycling in LiFePO<sub>4</sub> cells and suppressing dendrite formation. This multi-component strategy effectively reconciled the trade-off between mechanical reinforcement and ionic transport, extending beyond structural design alone.

Introducing a distinct approach, Guzmán-González et al.<sup>32</sup> developed methacrylic backbones bearing pendant borate groups (Figure 3i). The choice of substituent critically influenced performance; ethylene glycol-substituted borates provided the optimal balance, reaching a conductivity of  $1.65 \times 10^{-4}$  S cm<sup>-1</sup> at 60 °C, a transference number of 0.93, and stability up to 4.2 V. A crosslinked gel derivative further enhanced conductivity and enabled stable lithium cycling. In contrast, less solvating substituents restricted ion motion, underscoring the direct impact of pendant group chemistry on electrolyte performance.

Finally, Liang et al.<sup>33</sup> advanced polysiloxane-based SIPEs by grafting MASTFSiLi units onto polymethylsiloxane via thiol-ene chemistry (Figure 3j). Blending with poly(vinylidene fluoride-co-hexafluoropropylene) (PVDF-HFP) and incorporating carbonate plasticizers yielded free-standing membranes exhibiting conductivities of  $\sim 0.4$  mS cm<sup>-1</sup> at 20 °C and  $\sim 0.8$  mS cm<sup>-1</sup> at 40 °C, together with a wide electrochemical window ( $>4.8$  V). Both symmetric Li|Li and full Li|NMC cells demonstrated stable cycling and high-rate capability, in some cases outperforming liquid electrolyte counterparts at elevated currents. This work highlighted the promise of polysiloxane backbones as flexible yet mechanically robust hosts for high-performance solid polymer electrolytes.



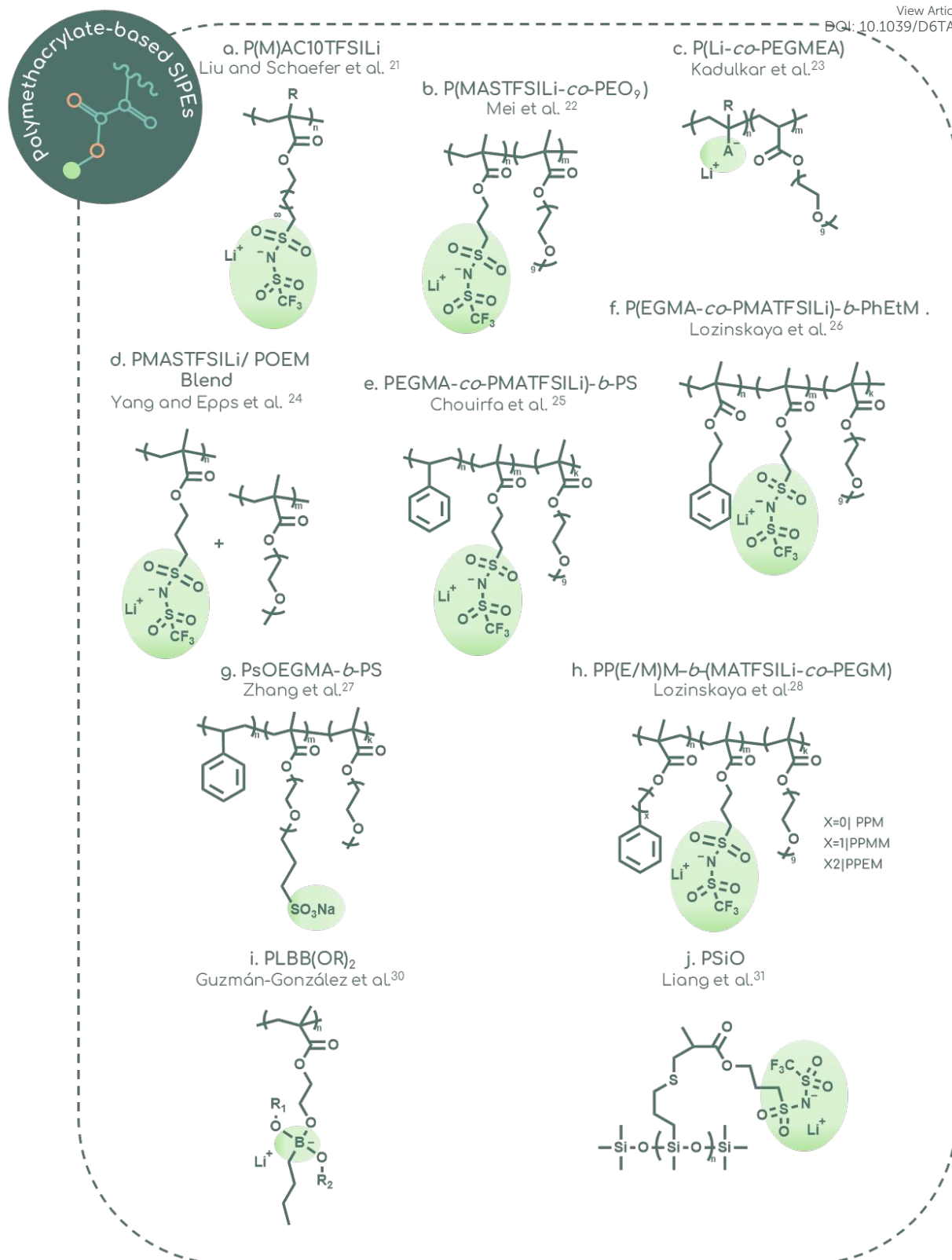


**Figure 3.** Overview of the chemical structures of methacrylate-based single-ion polymer electrolytes discussed in Section 2.2. The highlighted regions denote the pendant ion-bearing groups, illustrating the structural diversity of the ionic moieties linked to the polymer framework.



In methacrylate-based SIPEs, ion transport is governed by a delicate interplay among anion identity, local polarity, and mesoscale morphology. The studies discussed here collectively show that sulfonylimide-type anions generally outperform more localized sulfonate motifs, while ordered morphologies such as lamellae or continuous ionic nanochannels can improve both transport continuity and mechanical integrity. At the same time, excessive rigidity, overloading of ionic groups, or poorly controlled self-assembly can suppress mobility and reduce processability. Therefore, the main design lesson for methacrylate systems is that chemical versatility alone does not guarantee performance; rather, the most successful materials combine charge-delocalized anions with controlled phase organization and sufficient local free volume to support lithium motion.

### 2.3 Polyether-based SIPEs

Polyether backbones offer exceptional segmental flexibility, low glass transition temperatures, and strong lithium-ion coordination, making them foundational to the design of single-ion polymer electrolytes (SIPEs). Among them, poly(ethylene oxide) (PEO) is most commonly employed as a neutral, Li<sup>+</sup>-coordinating domain, whereas anionic functionalities are typically immobilized on more rigid polymer backbones or mechanically reinforcing segments, rather than on the polyether chain itself. However, the high crystallinity of PEO severely limits ionic conductivity under ambient conditions, and its poor mechanical integrity at elevated temperatures poses additional challenges. These limitations have driven the development of alternative polyether architectures that suppress crystallization and improve mechanical robustness, as well as design strategies in which PEO itself is functionalized to serve as the anion-bearing backbone, enabling tighter control over anion localization, ion-polymer interactions, and overall single-ion transport efficiency.

Hatakeyama-Sato et al.<sup>34</sup> grafted TFSILi or imidazolium groups onto a poly(allyl glycidyl ether) backbone via thiol-ene chemistry, achieving low glass transition temperatures (<0 °C) and room-temperature ionic conductivities up to 10<sup>-6</sup> S cm<sup>-1</sup> without the use of plasticizers. Uniform tethering of ionic groups, coupled with the inherent flexibility of the backbone, facilitated efficient single-ion conduction, underscoring the role of backbone mobility in ion transport (Figure 4a).

Taking a distinct approach, Dreier et al.<sup>35</sup> covalently attached trifluoromethanesulfonamide anions directly to the PEO segment of a polystyrene - polyethylene oxide block copolymer (PS-*b*-PEO), shifting the design focus from grafted polyethers to single-ion architectures integrated within mechanically robust frameworks (Figure 4b). The rigid polystyrene block imparted



structural integrity and oxidative stability, while the functionalized PEO segment maintained segmental flexibility and high  $\text{Li}^+$  mobility. By localizing anions within the PEO domains, this study achieved a balance between mechanical strength and ion transport, demonstrating how deliberate control over backbone composition and anion placement can jointly govern SIPE performance.

Further advances employed orthogonal post-polymerization modifications to develop highly tunable polyether-based single-ion conductors. By introducing allyl and hydroxyl functionalities along the backbone and subsequently grafting TFSILi groups together with triethylene glycol pendants (Figure 4c), researchers produced SIPEs featuring weakly coordinating, charge-delocalized anions and flexible  $\text{Li}^+$ -solvating side chains<sup>36</sup>. The incorporation of triethylene glycol pendant groups lowered the glass transition temperature, enhanced segmental and ion-rearrangement mobility, and increased the density of ion-conducting sites, resulting in approximately a 250-fold enhancement in ionic conductivity at 60 °C relative to the unmodified backbone ( $1.7 \times 10^{-6} \text{ S cm}^{-1}$  and  $6.7 \times 10^{-9} \text{ S cm}^{-1}$ , respectively).

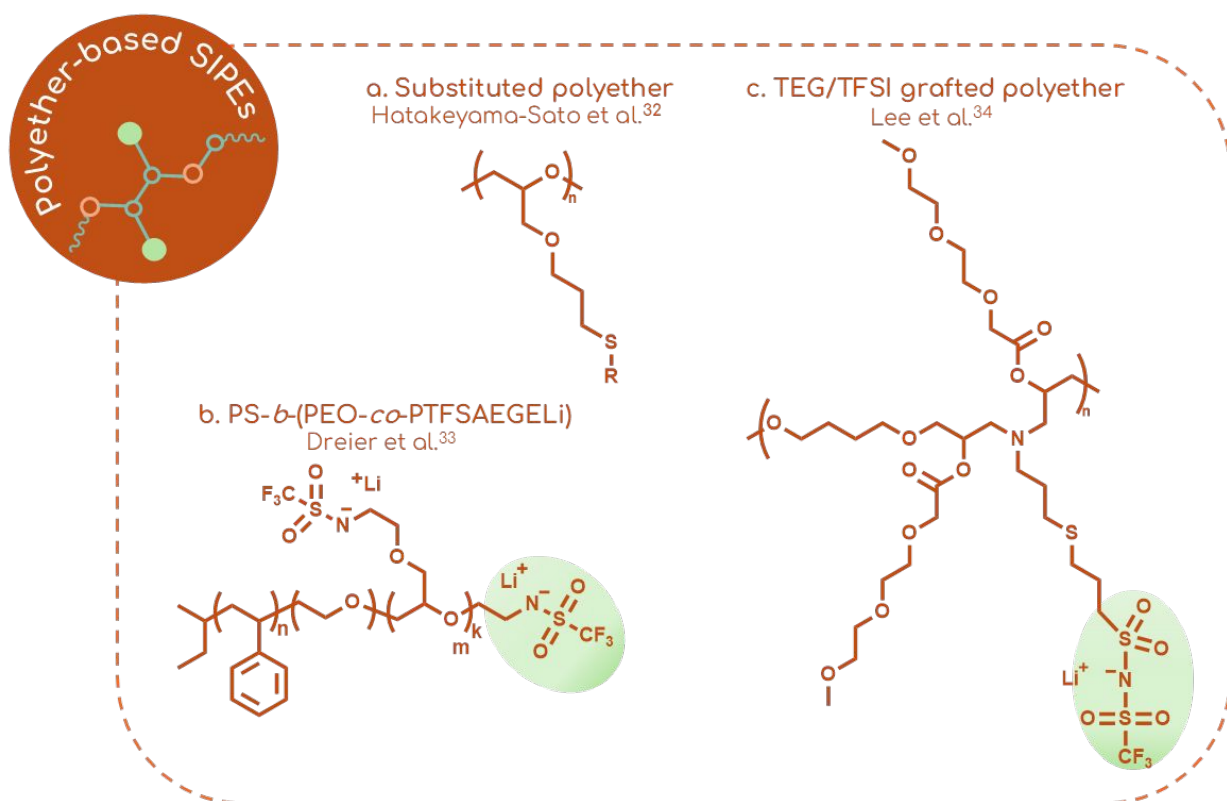


**Figure 4.** Overview of the chemical structures of polyether-based single-ion polymer electrolytes discussed in Section 2.3. The highlighted regions mark the pendant ion-bearing groups, highlighting variations in the ionic groups.



Polyether-based SIPEs confirm the central importance of segmental flexibility and Li<sup>+</sup> coordination, but also highlight the persistent limitations imposed by crystallization and weak mechanical strength. Across these examples, the highest-performing designs are those that either suppress crystallinity through chemical modification or embed polyether segments within more robust architectures that preserve mobility without sacrificing dimensional stability. Functionalization of polyether chains with charge-delocalized anions and solvating side groups further demonstrates that polyethers can serve not only as passive transport media but also as active structural components in single-ion conduction. Taken together, this family shows that the value of polyether chemistry lies in its transport efficiency, provided that crystallinity and mechanical fragility are structurally controlled.

#### 2.4 Aromatic backbone chemistry: Ketone and Sulfone-based SIPEs

Aromatic backbones such as aryl ether ketones, poly(ether sulfones), and diphenyl sulfones provide exceptional thermal and mechanical stability but often suffer from limited segmental mobility due to their rigidity. These polymers, typically synthesized via polycondensation or nucleophilic substitution, enable precise incorporation of ion-conducting moieties, making them strong candidates for durable, high-performance lithium battery electrolytes.

Jing et al.<sup>37</sup> addressed the mobility limitation by developing PSBILi (Figure 5a), a single-ion polymer electrolyte with an aromatic polyamide backbone and a high density of tethered lithium ions. Blending PSBILi with PVDF-HFP yielded porous membranes with enhanced solvent uptake and mechanical strength, resulting in improved ionic conductivity ( $\sim 10^{-4}$  S cm<sup>-1</sup> at 25 °C) and a Li<sup>+</sup> transference number near 0.9. The interconnected porosity promoted rapid Li<sup>+</sup> transport while maintaining sufficient mechanical strength to suppress dendrite formation.

To simplify fabrication while maintaining uniform ion distribution, Hu et al.<sup>38</sup> synthesized poly(2,2'-(ethylenedioxy)bis-(ethylamine), (4,4' -dicarbonyl benzene sulfonyl) bisimide), PEBILi, a bis(sulphonyl)imide-based polymer rich in ethylenedioxy groups (Figure 5b) and employed it as a functional filler within a PEO matrix. The resulting composite membranes exhibited reduced crystallinity, enhanced ionic conductivity of  $4.17 \times 10^{-4}$  S cm<sup>-1</sup> at 60 °C, and a lithium-ion transference number of 0.45. Despite the lower  $t_{Li^+}$ , the composite electrolytes enabled scalable processing, homogeneous lithium distribution, and stable lithium plating/stripping, supporting both high-rate cycling and long-term capacity retention in Li||LiFePO<sub>4</sub> cells.

Jagadesan et al.<sup>39</sup> pursued chemical modification to enhance ion dissociation by designing a copolymer which incorporated perfluorinated lithium-salt monomers covalently linked to polyethylene glycol units (AB-type, Figure 5c). The electron-withdrawing fluorine substituents



increased anion delocalization, yielding a conductivity of approximately  $10^{-4}$  S  $\text{cm}^{-1}$  at room temperature and a lithium-ion transference number of 0.92. The flexible PEG segments preserved mechanical integrity and when used in symmetric Li cells, facilitated uniform lithium deposition, mitigating concentration polarization and dendrite formation.

Further improvements in ionic density and backbone fluorination were explored by Dong et al.<sup>40</sup>, who designed a series of polysulfone-based single-ion polymer electrolytes (SIPes) membranes with systematically varied trifluoromethyl ( $-\text{CF}_3$ ) substitution and  $\text{Li}^+$  concentration (Figure 5d). The optimized composition, hexafluoropolysulfone-Li (6FPSF-Li) which featured the highest  $\text{CF}_3$  and  $\text{Li}^+$  content, exhibited an ionic conductivity of  $\sim 2.5 \times 10^{-4}$  S  $\text{cm}^{-1}$  at 40 °C, an anodic stability exceeding 4.8 V, and stable cycling in Li||NCM811 cells with high-mass-loading electrodes. These findings underscore that balancing fluorination degree and ionic content can maximize conductivity and electrochemical stability while preserving membrane processability.

Addressing high-voltage and low-temperature performance, Shi et al.<sup>41</sup> designed aromatic poly(ether sulfone) multiblock copolymers incorporating flexible segments to enhance  $\text{Li}^+$  mobility (Figure 5e). Plasticization improved lithium plating currents, suppressed dendrite formation, and maintained high anodic stability, demonstrating that integrating flexible domains can enhance low-temperature and rate capabilities without compromising mechanical strength. Finally, Li et al.<sup>42</sup> prioritized safety and lithium-ion selectivity by grafting STFSI groups onto a rigid poly(aryl ether ketone) (PAEK) backbone (Figure 5f). This design effectively decoupled  $\text{Li}^+$  transport from anion motion, achieving high transference numbers, conductivity around  $10^{-4}$  S  $\text{cm}^{-1}$  at 30 °C that improved as the temperature increased, and robust mechanical and thermal stability. Compared with the flexible and composite analogues examined in the same study, the rigid backbone offered superior structural and electrochemical resilience, albeit with limited segmental mobility at lower temperatures.

View Article Online  
DOI: 10.1039/D6TA01035K



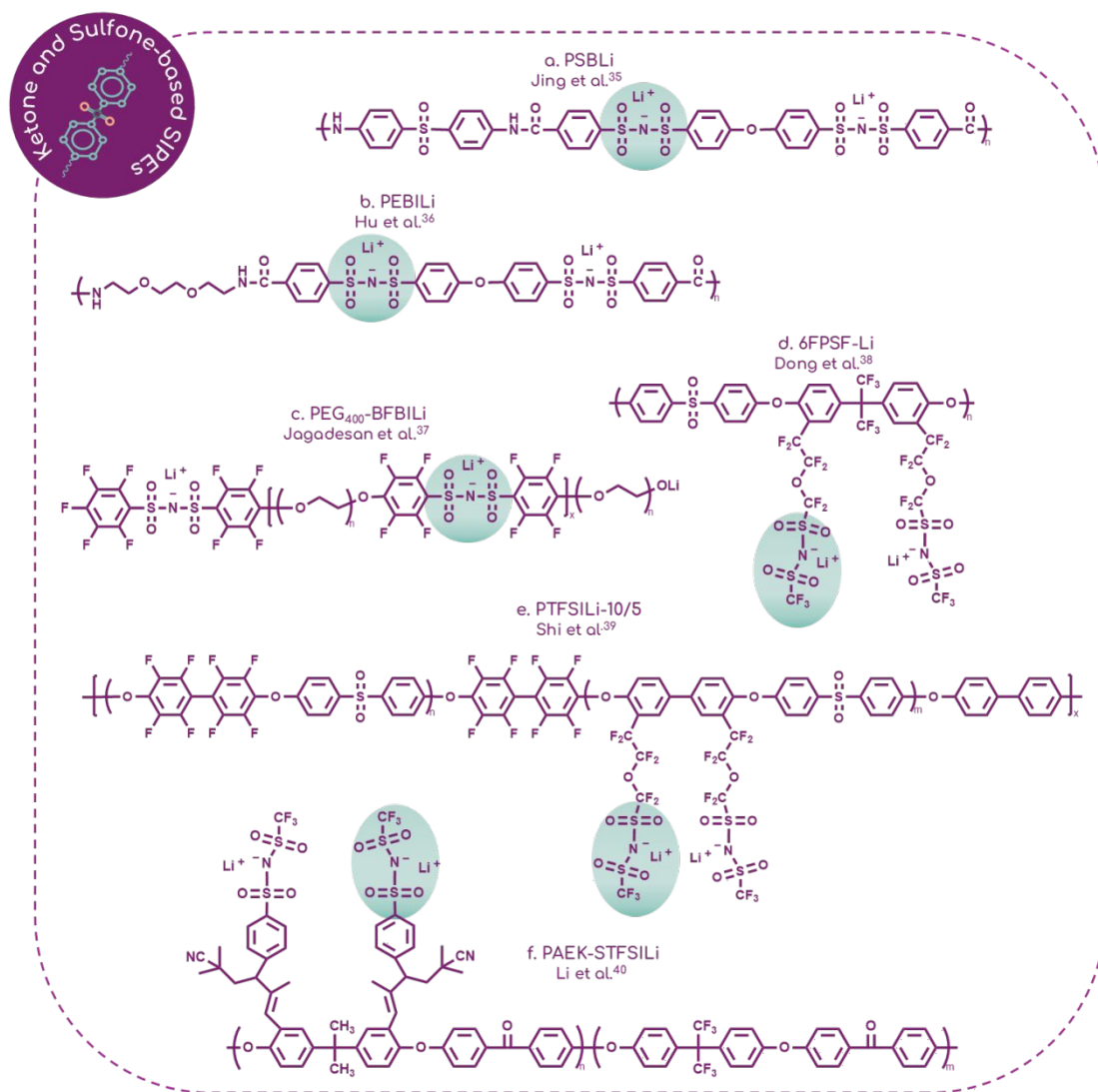


**Figure 5.** Overview of the chemical structures that employ aromatic-, ketone- and sulfone- based single-ion polymer electrolytes discussed in Section 2.4. The highlighted regions identify the pendant ion-bearing groups, underscoring the variation in ionic group chemistry attached to the parent polymer backbone.



Aromatic ketone- and sulfone-based SIPEs illustrate the opposite design philosophy to flexible polyether-rich systems: here, the backbone primarily contributes thermal, oxidative, and mechanical resilience, while ion transport must be recovered through porosity, flexible comonomers, plasticization, or highly delocalized anions. The reviewed studies show that these rigid frameworks are particularly attractive for high-voltage and mechanically demanding applications, but their conductivity is often limited unless mobility is reintroduced at the local or mesoscale level. Thus, the central structure–property relationship in this family is that backbone rigidity enhances stability and dendrite resistance, but requires compensatory design elements to avoid transport penalties. In practice, the most promising aromatic SIPEs are those that strategically combine rigid scaffolds with soft ion-solvating domains or morphology-engineered transport pathways.

## 2.5 Diverse backbone strategies

### 2.5.1 Zwitterions

The following studies highlight that zwitterionic architectures, achieved through grafting, doping, or hybrid crosslinked networks, can simultaneously promote ionic conductivity, lithium-ion selectivity, and mechanical durability, positioning them as highly promising candidates for next-generation solid-state lithium metal batteries.

Jones et al.<sup>43</sup> pioneered semicrystalline polymeric zwitterionic electrolytes (PZILs), in which covalently tethered zwitterions form ordered crystalline domains that act as ion-conducting channels (Figure 6a). This architecture decouples lithium-ion transport from polymer segmental motion, yielding conductivities of  $1.6 \text{ mS cm}^{-1}$  and lithium-ion transference numbers of 0.6–0.8 at room temperature, together with a broad electrochemical stability window ( $\sim 4.5 \text{ V vs Li/Li}^+$ ) and dendrite-free cycling.

Xu et al.<sup>44</sup> further advanced the concept by designing a polybiphenyl piperidinium (PBP) backbone dually grafted with PSiLi groups (Figure 6b), forming zwitterionic dipoles that increased dielectric permittivity, reduced ion aggregation, and achieved ionic conductivity of  $2.4 \times 10^{-4} \text{ S cm}^{-1}$  at  $25 \text{ }^\circ\text{C}$ , maintaining dendrite-free operation for over 2000 hours when employed in a symmetric Li cell. Similarly, Du et al.<sup>45</sup> synthesized a dually grafted polybenzimidazole (PBI-g-PSiLi, Figure 6c) membrane featuring a rigid aromatic backbone with high tensile strength ( $\sim 60 \text{ MPa}$ ), conductivity of  $\sim 0.15 \text{ mS cm}^{-1}$  at room temperature, and near-unity lithium-ion transference numbers, enabling stable lithium plating/stripping for over 1000 hours under galvanostatic cycling. Building upon this framework, Xu et al.<sup>46</sup> incorporated zwitterionic dopants into a dually grafted polybenzimidazole system (Figure 6c), further



enhancing room temperature conductivity to  $0.68 \text{ mS cm}^{-1}$ , achieving transference numbers up to 0.95, and sustaining long-term stability exceeding 2100 hours in symmetric Li|Li cells and 500 cycles in full cells.

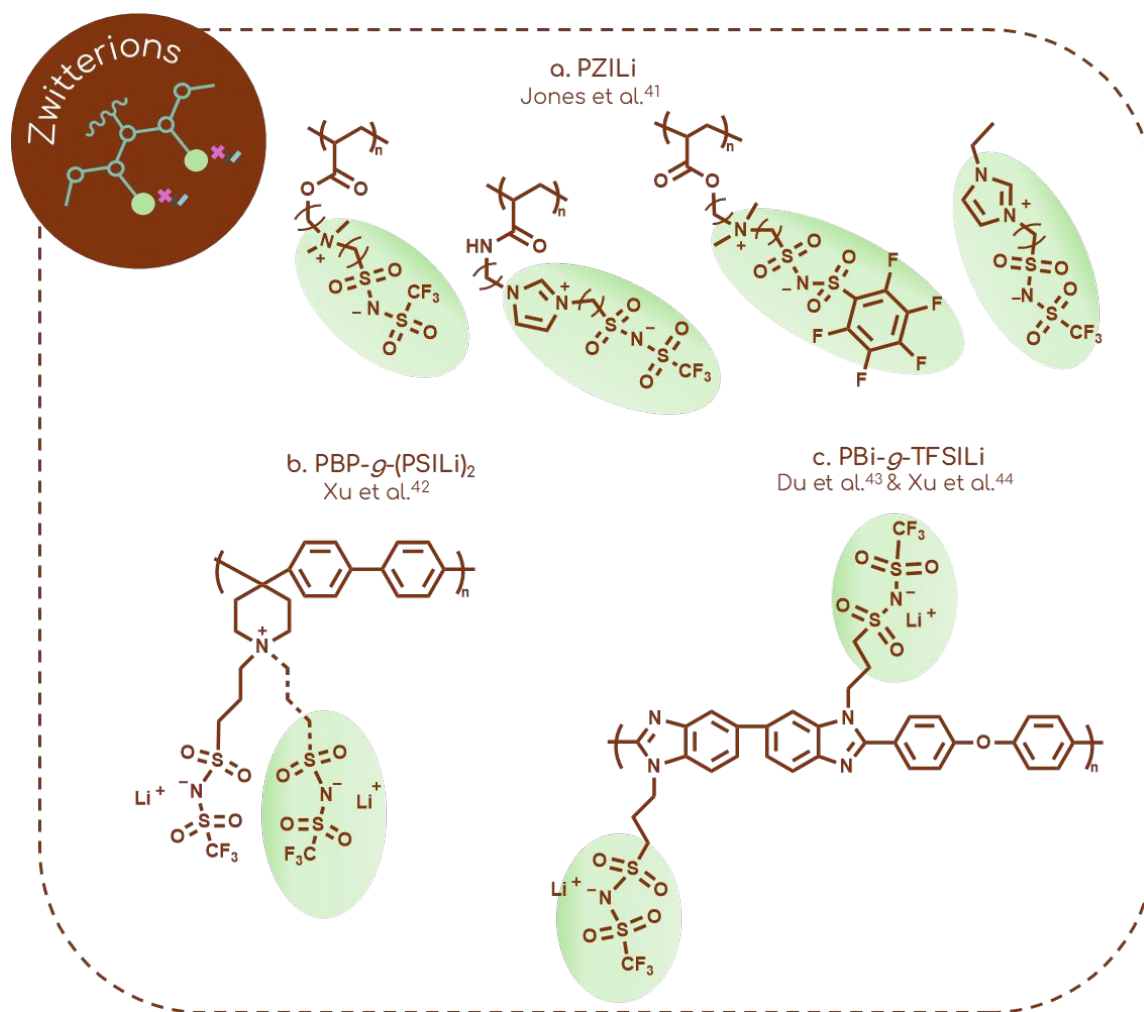


**Figure 6.** Overview of the chemical structures of zwitterionic single-ion polymer electrolytes discussed in Section 2.5.1. The highlighted regions denote the pendant ion-bearing groups, illustrating the structural diversity of the ionic functionalities.

Zwitterionic SIPEs stand out because they offer a route to simultaneously high conductivity, high lithium selectivity, and robust cycling stability without relying solely on conventional segmental transport mechanisms. The examples discussed suggest that zwitterionic dipoles increase dielectric screening, reduce ion aggregation, and in some cases promote partially decoupled ion transport, especially when combined with rigid aromatic backbones. Their main advantage lies in enabling high  $t_{\text{Li}^+}$  together with strong interfacial stability, while the main challenge remains balancing synthetic complexity with scalable processing. Overall, this subsection shows that zwitterionic design is a powerful molecular strategy for improving ion dissociation and long-term electrochemical stability in a single framework.



### 2.5.2 Polyethylene-based SIPEs

Polyethylene backbones provide a robust and adaptable framework for incorporating diverse ionic functionalities, making them highly effective scaffolds for designing high-performance single-ion conducting polymer electrolytes in lithium battery systems.

Zhang et al.<sup>47</sup> introduced a flexible platform through the development of a family of polyanions synthesized via nucleophilic aromatic substitution and ring-opening metathesis polymerization (Figure 7a). This design enabled precise tuning of electronic properties and sidechain spacing, allowing systematic control over ion dissociation and polymer-ion interactions. The resulting materials exhibited high ionic conductivity ( $10^{-4}$  S cm<sup>-1</sup> at 80 °C), strong cation selectivity ( $t_{\text{Li}^+}(\text{NMR})=0.79$ ), and high oxidative stability, demonstrating how rational side-chain engineering can simultaneously optimize transport and stability.

Building on polymer blending strategies, Nguyen et al.<sup>48</sup> functionalized a polyethylene backbone with spatially isolated TFSI groups to investigate miscibility with PEO, forming amorphous phases that achieved near-unity lithium-ion transference numbers. Similarly, Paren et al.<sup>49</sup> expanded on this approach by blending similar polyanions with low-molecular-weight PEO (Figure 7b), observing partial decoupling lithium-ion motion from polymer segmental relaxation. Together, these studies underscore how tailored backbone functionalization and controlled blending can harmonize conductivity and structural compatibility.

A morphology-driven strategy was pursued by Park et al.<sup>50</sup>, who designed segmented multiblock copolymers with alternating ionic and crystalline domains (Figure 7c). Selective solvation of the ionic layers using DMSO increased the concentration of free Li<sup>+</sup>, enhancing conductivity by four orders of magnitude ( $\sim 10^{-6}$  S cm<sup>-1</sup> at  $\sim 70$  °C of the solvated sample compared to the dry state) while preserving lamellar ordering. This work highlighted the pivotal role of nanoscale structural organization in facilitating efficient ion transport.

Finally, Fraile-Insagurbe et al.<sup>51</sup> focused on mechanical reinforcement by grafting lithium bearing functional groups onto a polyethylene-alt-maleimide backbone (Figure 7d) and blending the resulting polymer with PEO/PEGDME. The composite membranes exhibited exceptional toughness, dendrite resistance, and stable lithium plating/stripping in Li|Li cells, while full-cell LiFePO<sub>4</sub> performance was limited by relatively low ionic conductivity and progressive impedance growth. Although interfacial degradation limited long-term capacity retention, this approach demonstrated that mechanical robustness and ionic conductivity can be effectively co-optimized within a unified material platform, although further improvements in room-temperature transport and interfacial stability remain necessary.



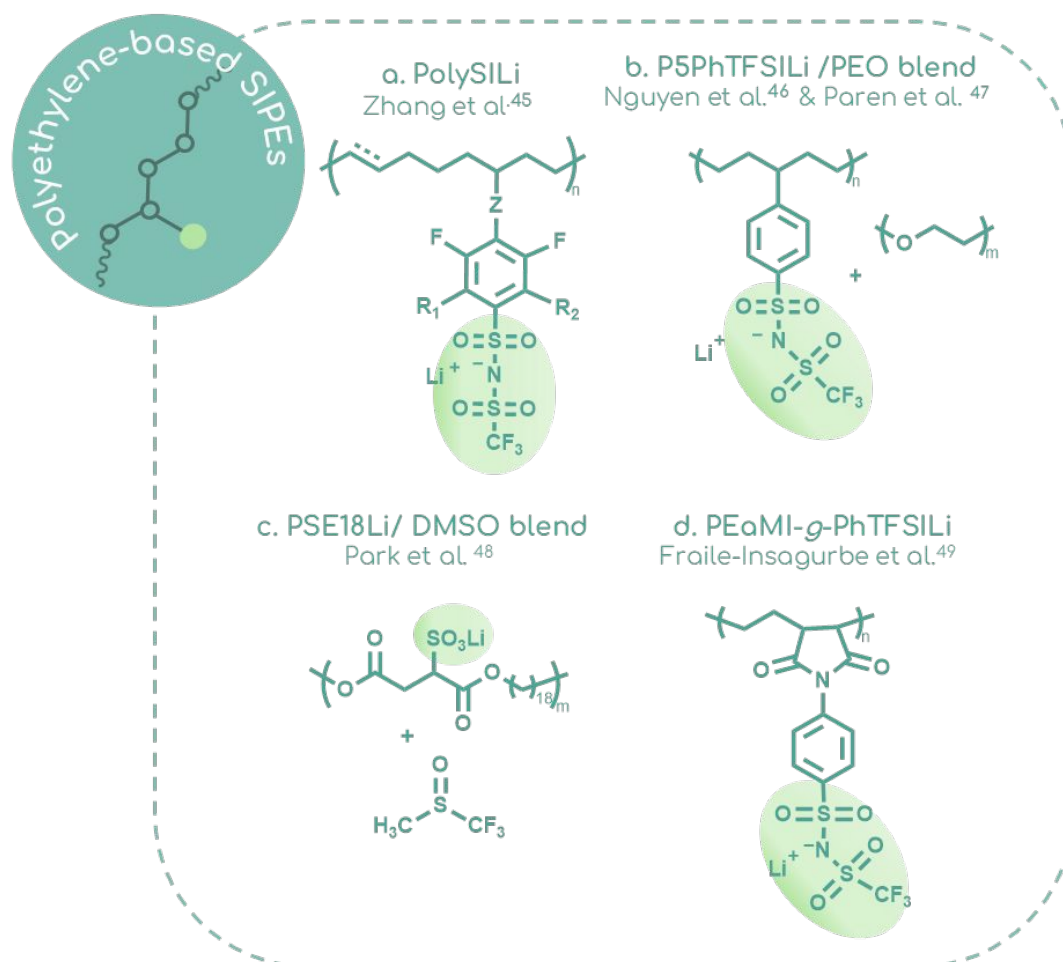


**Figure 7.** Overview of the chemical structures of polyethylene-based single-ion polymer electrolytes discussed in Section 2.5.2. The highlighted regions indicate the pendant ion-bearing groups, emphasizing differences in the ionic moieties attached to the polymer backbone.

Polyethylene-based SIPEs demonstrate that relatively simple hydrocarbon backbones can become highly effective single-ion platforms when side-chain chemistry and blend compatibility are carefully engineered. Across these studies, ionic dissociation, miscibility with PEO-like transport phases, and nanoscale organization emerge as the main determinants of performance, while mechanical reinforcement can be introduced without completely sacrificing ion mobility. However, the battery-level results also show that stronger membranes do not automatically translate into durable full-cell operation if interfacial impedance remains poorly controlled. The key lesson from this family is that polyethylene scaffolds are highly adaptable, but their success depends on converting a mechanically robust framework into one that also supports continuous and sufficiently solvated lithium transport.

### 2.5.3 Polyurethane-based SIPEs



Polyurethane-based single-ion polymer electrolytes (SIPes) have been explored through a range of synthetic strategies, each seeking to balance ionic conductivity with mechanical robustness. In a recent study, Wang et al.<sup>52</sup> designed polyurethane–urea systems with immiscible rigid aromatic urethane and flexible poly(ethylene oxide) segments (Figure 8a), forming microphase-separated architectures in which increasing the hard segment content enhanced mechanical strength (up to 11 MPa) but restricted segmental mobility, leading to reduced ionic conductivity ( $\sim 2.4 \times 10^{-6} \text{ S cm}^{-1}$  at 80 °C under high ionic loading). In a subsequent study on polyurethane–ester (PUE) systems<sup>53</sup> (Figure 8b), the authors optimized phase separation by tuning the PEG chain length and hard-phase composition, achieving ionic conductivity of around  $10^{-4} \text{ S cm}^{-1}$  at 80 °C with the use of carbon-based plasticizers, high tensile strength (13.6 MPa), and stable cycling performance in lithium-metal batteries. However, this system required precise control to prevent phase instability and ion aggregation. A complementary approach<sup>54</sup> employed sulfonamide-functionalized polyurethanes, in which bulky anions were introduced into the hard phase to generate ion-conductive nanochannels (Figure 8c). The optimized plasticized membrane achieved  $1.1 \times 10^{-4} \text{ S cm}^{-1}$  at 30 °C with a near-unity lithium-ion transference number. At higher ion concentrations, incorporation of bulky sulfonamide groups disrupted hard-domain ordering, necessitating composition optimization to preserve mechanical integrity.

View Article Online  
DOI: 10.1039/D6TA01035K



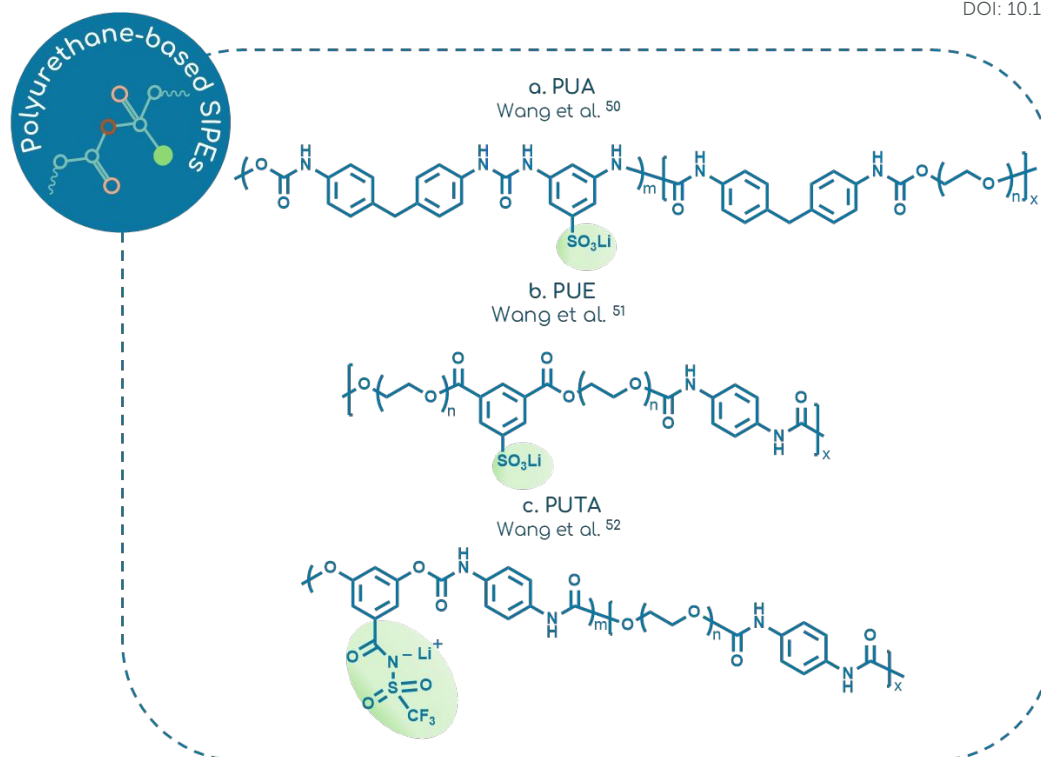


**Figure 8.** Overview of the chemical structures of polyurethane-based single ion polymer electrolytes discussed in Section 2.5.2. The highlighted regions indicate the pendant ion-bearing groups, illustrating differences in the ionic moieties appended to the macromolecular scaffold.

Collectively, these studies illustrate that enhancing ionic conductivity typically requires increasing soft-segment content and promoting ionic dissociation, often at cost of mechanical stability. Conversely, reinforcing mechanical properties through greater hard-domain regularity can impede ion transport. These findings underscore the importance of rationally engineered multiphase architectures that balance electrochemical performance with mechanical durability in next-generation lithium battery electrolytes.

### Overall Structure–Property–Performance Trade-Offs in Linear SIPEs

In linear SIPEs, the dominant structure–property–performance relationship is set by backbone chemistry and the local ionic environment. Flexible, polar, and weakly coordinating structures generally promote ion-pair dissociation, segmental motion, and thus higher ionic conductivity, whereas rigid aromatic frameworks and mechanically reinforcing motifs improve dimensional integrity, oxidative stability, and resistance to lithium dendrite penetration, often at the cost of reduced chain mobility and lower conductivity. Across the linear systems discussed here, high performance therefore does not arise from maximizing a single property, but from balancing several competing requirements: sufficient local mobility for  $\text{Li}^+$  transport, adequate charge



delocalization of the tethered anion, morphological stability under operation, and compatibility with practical processing and battery interfaces. In this context, the most promising linear SIPEs are those that use chemistry not only to enhance conductivity, but also to moderate the usual penalties in mechanical robustness and electrochemical stability, thereby defining a more balanced route toward battery-relevant performance.

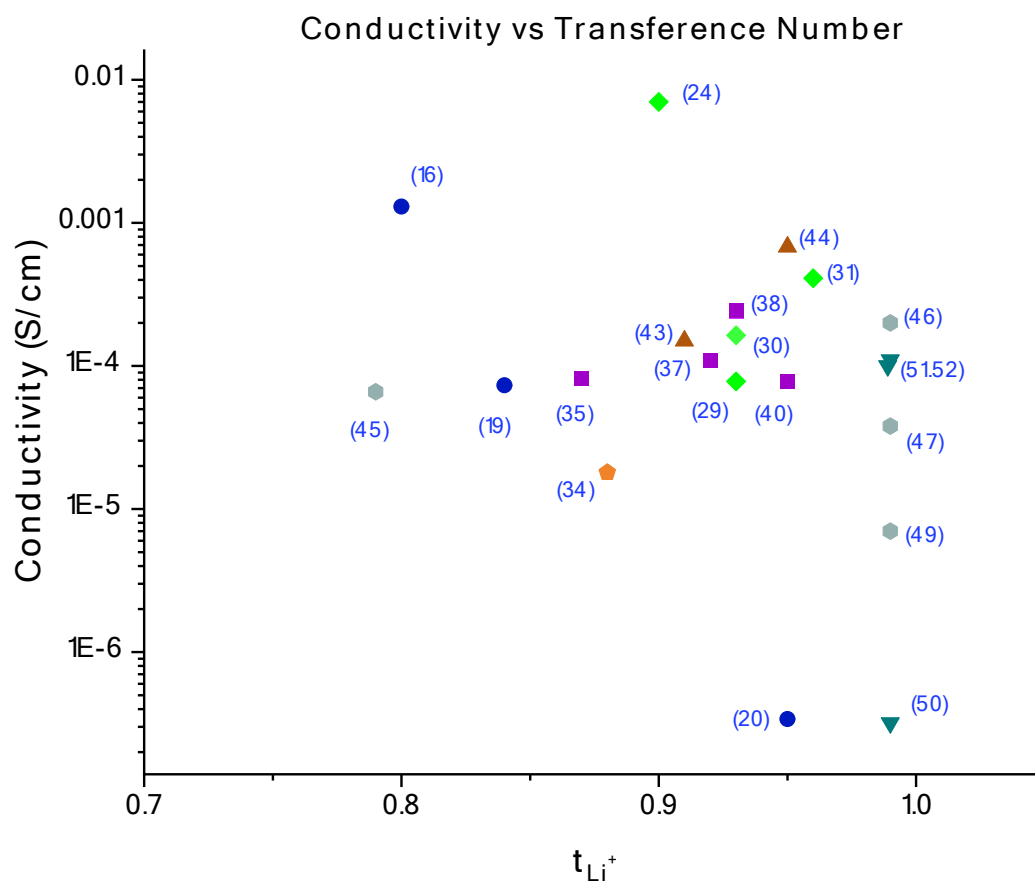


**Figure 9.** Conductivity vs  $t_{Li^+}$ , for linear systems. Each symbol/ color represents the different backbone chemistry [● Polystyrene-based, ◆ Polymethacrylate-based, ◆ Polyether-based, ■ Aromatic backbones, ▲ Zwitterions, ● Polyethylene-based & ▼ Polyurethane-based SIPEs.

### 3. Non-linear polymer systems: Architecture-driven properties

Linear systems are primarily governed by polymer chain segmental motion and local chemical environment, whereas non-linear systems introduce additional degrees of freedom, such as spatial constraints, nanoscale phase separation, and interfacial effects, which enable alternative strategies for tuning ion transport and mechanical properties. In contrast to the chemistry-driven classification of linear SIPEs, the following section organizes non-linear systems according to their macromolecular architecture and material design strategies. These approaches, spanning



miktoarm stars, nanoparticle-based systems, brushes and network-forming electrolytes, illustrate how architectural complexity can be harnessed to simultaneously improve ion transport, mechanical rigidity or flexibility, and processing practicality. By focusing on complex macromolecular architecture rather than specific chemical moieties, this framework reflects the integrated design philosophy required for realistic solid-state electrolyte development, where a single material must satisfy multiple, often competing, performance criteria.

### 3.1 Prioritizing Ion Transport and Electrochemical Stability: Electrochemical Performance as the Core Target

In the development of high-performance solid polymer electrolytes (SPEs), enhancing ionic conductivity and lithium-ion selectivity remains a central design objective. Among non-linear macromolecular systems, architectures that introduce topological confinement, dynamic heterogeneity, or ion-tethering mechanisms have proven especially effective. The following studies highlight how single-ion star-shaped polymers, single-ion polymer nanoparticles, crosslinked polymer networks, and UV-cured materials employ architectural design to optimize ion transport and improve electrochemical stability (Figure 9, Table 1).

Bocharova et al.<sup>55</sup> introduced single-ion conducting hairy nanoparticles (NPs), consisting of a SiO<sub>2</sub> core grafted with poly(MTFSILi) chains (Figure 9a), as additives for PEO–TFSILi electrolytes. Both hairy NPs and their linear analogue (PolyIL) are intrinsically poor conductors due to their high T<sub>g</sub> values (201 and 190 °C, respectively), but when incorporated into the dual-ion conductive PEO–TFSILi matrix (Li/EO = 0.051) at loadings up to 9.1 wt.%, they produced markedly different effects. PolyIL strongly disrupted PEO crystallinity, whereas hairy NPs intercalated primarily into amorphous regions, largely preserving semi-crystallinity. At higher NP contents, segmental mobility decreased, lowering conductivity (0.26 mS cm<sup>-1</sup> at 60 °C for Hairy\_10, with 9.1 wt.% particle loading, vs. 4.1 × 10<sup>-4</sup> S cm<sup>-1</sup> for neat PEO–TFSILi) and reducing t<sub>Li+</sub>. However, this reduced mobility also translated into enhanced mechanical strength (0.46 MPa at 60 °C for Hairy\_10), supporting bulk and interfacial stability. As a result, hairy NPs significantly enhanced cycling stability of Li|Li symmetric cells, with Hairy\_5 (4.8 wt.% particle loading) and Hairy\_10 (9.1 wt.% particle loading) remaining stable for ~340 h at 0.2 mA cm<sup>-2</sup> and 0.20 mAh cm<sup>-2</sup>, and under extended cycling at 1.0 mAh cm<sup>-2</sup>, Hairy\_10 maintained performance for an additional ~150 h while Hairy\_5 failed rapidly. These results demonstrate that hairy NP additives, by improving homogeneity and interfacial stability, can substantially extend the cycling life of dual-ion PEO-based electrolytes.

View Article Online  
DOI: 10.1039/D6PA01035K



Moving from nanoparticle additives to star-shaped copolymers, researchers have also explored architectures where conducting and ion-bearing phases are confined together within the same molecular framework. Pantazidis et al.<sup>56</sup> reported the synthesis of miktoarm star copolymers composed of PEO and poly(STFSILi) (PSTFSILi) arms from a PDVB core using an “arm-first, in-out” approach (Figure 9b). The resulting stars had ~22 arms of each type, and the Li/EO ratio was systematically tuned ( $r$ : 0.046–0.204) by varying PSTFSILi chain length. Unlike linear block copolymers, which tend to microphase-separate and trap ions, the miktoarm configuration ensured molecular-level miscibility, suppressing crystallization and maintaining amorphous character even at low salt content ( $r \geq 0.046$ ). This architecture promoted efficient ion dissociation, reflected in a strong increase of  $T_g$  with higher ionic content (–20 to ~60 °C). Conductivity decreased monotonically with increasing PSTFSILi chain length (higher  $r$ ), as the volume fraction of the PEO phase diminished. The best-performing sample, PEO(105)\_PSTFSILi(4.8) (averaging 105 units of PEO and 4.8 units of TFSILi per arm,  $r = 0.046$ ), reached conductivities on the order of  $10^{-5}$  S cm<sup>-1</sup> at 90 °C, representing a gain of about seven orders of magnitude compared to earlier PEO/PSTFSILi miktoarm stars with POSS cores<sup>57</sup>. This work exemplifies how careful topological control can couple amorphicity, miscibility, and ion dissociation to yield single-ion conductors with significantly enhanced transport performance.

From well-defined star systems and nanoparticles, attention has also turned to crosslinked networks where connectivity and rigidity can be tuned to balance conductivity and ion selectivity. Chen et al.<sup>58</sup> reported the synthesis of slightly cross-linked single-ion conducting networks based on alternating copolymers containing grafted ethylene glycol oligomers and pendant 4-styrenesulfonyl(4-(trifluoromethoxy)benzenesulfonyl)imide (SSTFMBSI<sup>-</sup>) anionic groups (Figure 9c). By incorporating flexible mPEG side chains and cross-linking via diamino-PEG linkers, the resulting materials exhibited tunable Li/EO ratios (0.073–0.089) and formed robust, self-standing films. The alternating distribution of solvating ethylene glycol units and immobilized anions strongly suppressed PEO crystallinity (4.4–7.8%), compared to >50% crystallinity in simple PEO blends, yielding largely amorphous electrolytes. This morphology enabled efficient Li<sup>+</sup> transport, with room-temperature ionic conductivities of  $10^{-6}$ – $10^{-5}$  S cm<sup>-1</sup> and high transference numbers ( $t_{Li^+} = 0.87$ – $0.91$ ). The degree of cross-linking was found to be critical; looser networks allowed some mobility of anionic chains under strong electric fields, reducing selectivity, whereas optimized cross-linking (C-ASPE-5/8, a cross-linked alternating single-ion polymer electrolyte where 5 out of every 8 maleic anhydride sites are reacted with diamino-PEG cross-linker) balanced conductivity and  $t_{Li^+}$ . Electrochemical testing



demonstrated excellent cycling stability: Li|Li symmetric cells at 40 °C (just above  $T_m$ ) showed low polarization ( $\sim 0.18$  V) for 350 h without dendrite formation, while full LiFePO<sub>4</sub>|Li cells retained 89% of their initial 137.7 mAh g<sup>-1</sup> capacity after 100 cycles at 0.1 C. The results highlight how alternating anion/solvation segment design coupled with controlled cross-linking yields single-ion polymer electrolytes with both high Li<sup>+</sup> selectivity and stable long-term cycling.

Extending this strategy, UV-cured systems have been developed as a facile route to free-standing membranes, combining structural integrity with tailored conductivity and interfacial stability. Liang et al.<sup>59</sup> developed photo-cross-linked single-ion polymer electrolytes (PSIPes) using UV-initiated radical polymerization of lithium (3-methacryloyloxypropylsulfonyl)(trifluoromethoxy-sulfonyl)imide (MTFSILi) with pentaerythritol tetraacrylate (PETA) as cross-linker, followed by hot pressing to yield smooth, self-standing membranes (Figure 9d). A MTFSILi:PETA ratio of 2:1 was identified as optimal, providing high conductivity while maintaining mechanical integrity, whereas 3:1 produced brittle membranes and 1:1 gave significantly lower conductivity. Although the network exhibited a low  $T_g$  ( $-29$  °C), further enhancement of Li-ion mobility was achieved by incorporating 80 wt.% propylene carbonate (PC) as plasticizer. The swollen membranes displayed Vogel–Tammann–Fulcher behavior, indicating Li<sup>+</sup> transport coupled to segmental dynamics and supported by PC coordination, with ionic conductivities of  $2.1 \times 10^{-4}$  S cm<sup>-1</sup> at 20 °C and  $4 \times 10^{-4}$  S cm<sup>-1</sup> at 40 °C. Importantly, Li|Li symmetric cells cycled for 1000 h with no increase in overpotential, demonstrating excellent stability against lithium metal. These results underscore the promise of PSIPes as EO-free, single-ion conductors that combine high conductivity with remarkable interfacial stability.

He et al.<sup>60</sup> demonstrated that anion-tethered single-ion conductors (SICs) can simultaneously achieve practical conductivity and morphological stabilization of Li metal, overcoming a common limitation of SIC systems. Using a single-step, solvent-free UV polymerization approach, they synthesized networks (Figure 9e) from trifluoromethanesulfonylimide lithium methacrylate (LiMTFSILi), ethylene acrylate (EA), and ethylene glycol dimethyl acrylate (EDA), with PEG<sub>250</sub> as plasticizing matrix (15.4–61.5 wt.%). PEG<sub>250</sub> usage greatly enhanced chain segmental mobility, lowering  $T_g$  from 8.3 °C to  $-77.2$  °C and reducing the activation energy for ion conduction ( $7.72$  kJ mol<sup>-1</sup>). The optimized SIC (SIC-3) reached ionic conductivities of  $7.4 \times 10^{-5}$  S cm<sup>-1</sup> at 30 °C and  $1.9 \times 10^{-5}$  S cm<sup>-1</sup> at 60 °C. Crucially, covalently tethered anions afforded a high transference number ( $t_{Li^+} = 0.85$ ), compared to 0.39 for the analogous dual-ion conductor (DIC-1), despite its higher conductivity. This selective ion



transport translated into superior electrochemical stability where SIC-3 sustained a three-fold higher critical current density (2.4 vs. 0.8 mA cm<sup>-2</sup> for DIC-1) and enabled smooth, whisker-free Li deposition. Li|Li symmetric cells cycled stably for 1000 h with constant overpotential (~100 mV), underscoring the role of anion immobilization in mitigating concentration polarization and suppressing dendrite growth.

From homogeneous cross-linked networks, efforts have also expanded toward interpenetrating hybrid electrolytes, where inorganic components such as POSS further tailor stability and ion transport. In a recent study<sup>61</sup>, a series of POSS-containing 3D crosslinked semi-interpenetrating single-ion hybrid polymer electrolytes (SINHEs, Figure 9f) was developed by UV-initiated polymerization of MATFSILi with methylacryl-POSS in the presence of PVDF-HFP, followed by swelling in EC/DEC (1:1 v/v). The base system, a single-ion polymer electrolyte (SIPE), ensures that only Li<sup>+</sup> is mobile, while anions are covalently tethered to the polymer backbone. Introducing the 3D crosslinked network (SINPE) already reduced crystallinity and enhanced segmental motion ( $T_g \approx -12.6$  °C vs  $-9.9$  °C for SIPE). Incorporation of POSS further disrupted polymer ordering, lowering  $T_g$  to  $\approx -26$  °C, while also boosting flexibility (tensile strength  $\sim 3.4$  MPa, elongation  $\sim 97\%$ ). The best-performing SINHEs achieved  $\sigma = 9.09 \times 10^{-5}$  S cm<sup>-1</sup> at room temperature with  $t_{Li^+} = 0.85$ , surpassing both SIPE and SINPE. This was attributed to faster polymer dynamics and the ability of Si–O cage structures in POSS to coordinate Li<sup>+</sup>, weaken Li–anion interactions, and open efficient ion transport channels, though excessive POSS content blocked conduction pathways and reduced conductivity. Electrochemical testing in Li|Li symmetric cells revealed improved cycling performance: traditional dual-ion polymer electrolyte (DINPE) cells short-circuited after  $\sim 140$  h due to dendrite growth, while linear SIPE cells showed interfacial degradation and rising polarization after  $\sim 600$  h. In contrast, the POSS-containing SINHEs cycled for over 2000 h at 0.1 mA cm<sup>-2</sup> with stable polarization and effective dendrite suppression, highlighting the role of POSS-containing SINHEs in improving interfacial stability and dendrite suppression.

Finally, moving beyond predominantly PEO-based frameworks, carbonate-based systems provide an alternative solvation chemistry that maximizes dissociation and selectivity while maintaining conductivity. Engler et al.<sup>62</sup> developed carbonate-based single-ion conducting polymer electrolytes (SICPEs) as an alternative to PEO-based hosts (Figure 9g), exploiting the electron-delocalized nature of cyclic carbonates to enhance Li<sup>+</sup> dissociation and provide intrinsic crosslinking sites. Among the copolymers screened, a dicarbonate acrylate–MTFSILi copolymer (MDCA67) exhibited the highest conductivity ( $1.7 \times 10^{-3}$  S cm<sup>-1</sup> at 75 °C) but insufficient mechanical robustness. To address this, the polymer was crosslinked with



PEGDMA and plasticized with vinylene carbonate (VC), yielding flexible gel electrolytes with drastically improved performance. The most optimized formulation (VC70, containing 70 wt.% VC) achieved ionic conductivity of  $0.16 \text{ mS cm}^{-1}$  at room temperature and an exceptional lithium transference number of 0.92, significantly outperforming the EC/DEC-plasticized analogue ( $t_{\text{Li}^+} = 0.66$ ,  $0.26 \text{ mS cm}^{-1}$ ). This translated into superior electrochemical stability; VC70 sustained 1000 h of stable Li|Li cycling at  $0.3 \text{ mA cm}^{-2}$  with suppressed overpotential hysteresis, while ECDEC70 suffered dendritic failure within  $\sim 100 \text{ h}$ . While the very high plasticizer content may compromise mechanical robustness and raise concerns for practical application, this study demonstrates that polycarbonate-based SICPEs, when combined with strong VC plasticization, can overcome the low conductivity of conventional SICs while ensuring highly selective ion transport and stable Li deposition.

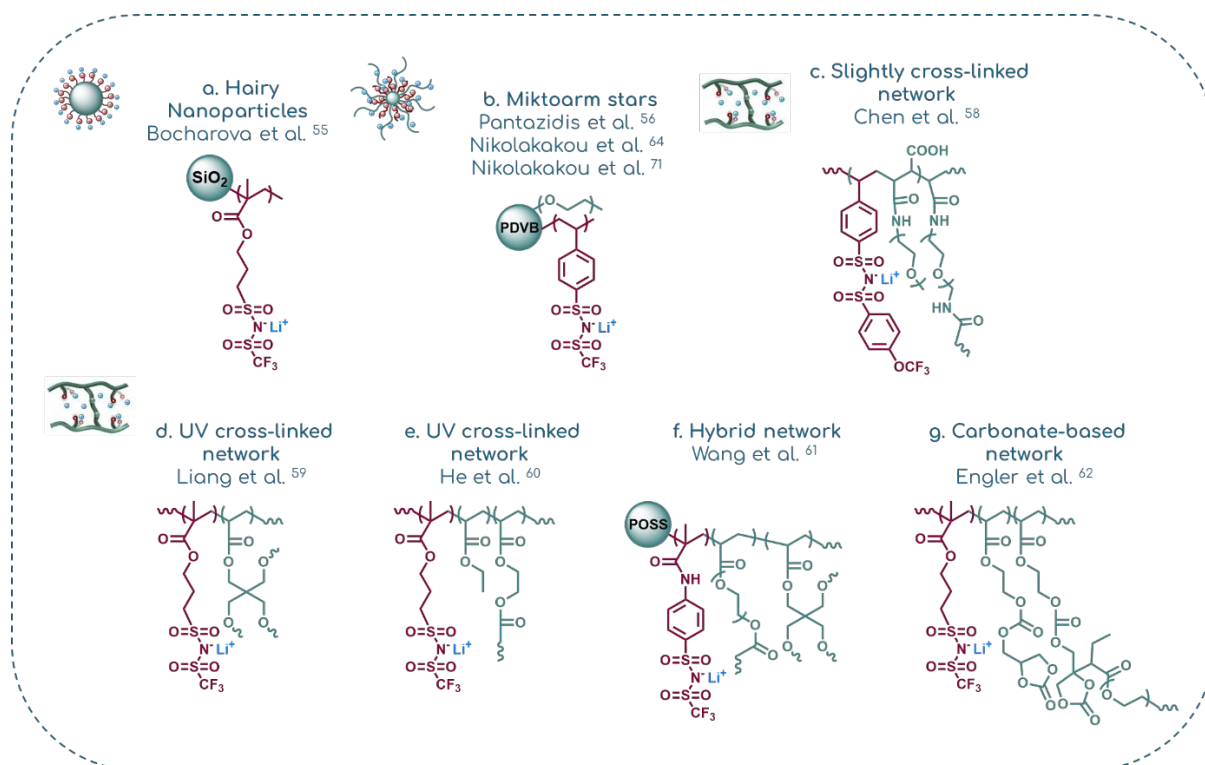


**Figure 10.** Chemical structures and the associated macromolecular architectures, for SIPE systems prioritizing ion transport and/or electrochemical stability. The representative architecture of each system is shown above its corresponding chemical structure, while the red-highlighted moieties indicate the ion-bearing groups and the green-highlighted segments correspond to the remaining polymer structure.



**Table 1.** Overall characteristics and remarks for non-linear SIPEs, that prioritize ion transport and/or electrochemical stability.

Reference No.	Preparation Method	Macromolecular architecture	Matrix	Lithium transference number, $t_{Li^+}$	Mechanical performance	Ionic conductivity ( $S\ cm^{-1}$ )	Remarks
55	RAFT polymerization from $SiO_2$ particle core	Hairy nanoparticles	Additives to PEO/LiTFSI	0.15 – 0.25	0.39 -0.46 MPa (Shear moduli, 60 °C)	$2.6 - 3.8 \times 10^{-4}$ (60 °C)	Improve cycling stability when used as additives
58	Prepolymer crosslinking, drop casted membranes	Slightly crosslinked network	-	0.91	3.63 – 4.43 MPa (Tensile strengths)	$1.96 \times 10^{-4}$ (30 °C)	Unique alternate structure of polymer backbone contributes to $Li^+$ distribution and transfer
59	UV initiated radical polymerization, hot pressed into self-standing membranes	Crosslinked network	Polymer network + Propylene Carbonate	-	-	$2.1 \times 10^{-8}$ (rt) – $4.0 \times 10^{-4}$ (40 °C)	Ion transport, Electrochemical stability
60	UV initiated free radical polymerization	Crosslinked network	PEG <sub>250</sub>	0.85	0.26 MPa (Tensile strength) 60 MPa (Storage modulus)	$7.44 \times 10^{-5}$ (rt) – $1.92 \times 10^{-4}$ (60 °C)	Efficient Ion transport Improved Morphological stability of Lithium Metal Anodes
61	UV initiated free radical polymerization	Interpenetrating network	EC/DEC	0.73-0.84	2.67 – 3.43 MPa (Tensile strength) Elongation at break: 78.5 – 97.2%	$5.94 - 9.09 \times 10^{-5}$ (rt)	Hybrid interpenetrating networks with POSS for enhanced conductivity, mechanics, and interfacial stability
62	RAFT polymerization, UV curing	Crosslinked network	Vinylene Carbonate	0.66 – 0.92	0.12 MPa (Tensile strength) 129 MPa (Storage modulus)	$10^{-9} - 10^{-4}$ (rt)	Dicarbonate monomers as promising alternatives to PEO



### 3.2 Focusing on Mechanical Integrity

View Article Online  
DOI: 10.1039/D6TA01035K

While previously mentioned examples focused on single-ion non-linear polymer designs have prioritized electrochemical stability to extend cycling life, long-term performance of lithium metal batteries also require materials capable of mechanically suppressing dendrite growth. Beyond optimizing interfacial transport and ion selectivity, introducing polymers with intrinsically high stiffness or incorporating reinforcing additives into otherwise conductive matrices provides an effective route toward robust, dendrite-resistant electrolytes. By moving away from systems that rely solely on electrochemical stabilization, these approaches demonstrate that mechanical integrity can be leveraged alongside conductivity, offering pathways to electrolytes that deliver both stable transport and strong resistance against morphological degradation of lithium anodes. The following examples illustrate this strategy (Table 2).

Porcarelli et al.<sup>63</sup> reported the synthesis of single-ion conducting polymer nanoparticles (LiPNPs) via a scalable semibatch emulsion polymerization, where MTFSILi comonomer was incorporated into cross-linked PMMA particles (Figure 10e), yielding sizes of 95–200 nm with  $\sim 5$  sulfonamide groups per  $\text{nm}^2$  on the surface. These LiPNPs were explored in two composite electrolyte systems, namely a dual-ion PEO-based composite and a single-ion PC-based gel. In the first, they were incorporated as nanofillers into high-molecular-weight PEO (900 k, 25 wt.% TFSILi), forming PEO–TFSILi–LiPNP composites. Loadings from 10–50 wt.% (PEO-NP10–50, number represents the wt. %) progressively stiffened the membranes ( $E'$  exceeding  $10^6$  Pa at 80 °C), while conductivity decreased with increasing filler content. The most conductive sample, PEO-NP10, reached  $1.0 \times 10^{-6}$  S  $\text{cm}^{-1}$  at 20 °C and  $6.6 \times 10^{-4}$  S  $\text{cm}^{-1}$  at 80 °C, while higher NP loadings (e.g., PEO-NP30) reduced conductivity by almost an order of magnitude. This reduction was attributed to increased tortuosity of the lithium-ion pathways caused by the presence of the particles, along with an overall decrease in the concentration of mobile ions. In the second case, LiPNPs were dispersed directly in propylene carbonate (20–60 wt.%, PC-NP20-60, number represents wt.%), producing single-ion conducting gels. Here, the mechanical properties scaled dramatically with NP content:  $G'$  rose from  $\sim 10$  Pa at 20 wt.% to  $\sim 10^6$  Pa at 60 wt.%, spanning several orders of magnitude. Conversely, ionic conductivity followed the opposite trend, with the most conductive samples, PC-NP20 achieving  $9.5 \times 10^{-5}$  S  $\text{cm}^{-1}$  at 25 °C and  $2.8 \times 10^{-4}$  S  $\text{cm}^{-1}$  at 85 °C, while PC-NP60 showed  $\sim 10^{-6}$  S  $\text{cm}^{-1}$  at 25 °C. Importantly, the gels reached a lithium transference number of  $t_{\text{Li}^+} \approx 0.8$ , confirming their near single-ion nature. Overall, this work highlights single-ion polymer nanoparticles as a versatile and scalable filler strategy to reinforce polymer electrolytes. They enable a tunable balance



between conductivity and mechanical integrity, offering promising design elements for dendrite-resistant electrolytes in lithium metal batteries.

While the above system emphasized nanoparticles as fillers to tune the conductivity–mechanical balance, the next work shifted focus back to miktoarm star copolymers, probing how molecular topology governs the interplay of modulus and ion transport. Following their earlier work on miktoarm stars<sup>56</sup>, Nikolakakou et al.<sup>64</sup> extended the study to probe the relationship between ionic conductivity and mechanical modulus in single-ion conducting polyanion miktoarm star copolymers composed of poly(styrene-4-sulfonyltrifluoromethylsulfonyl)imide lithium (PSTFSILi) arms that are a complement to longer ion-conducting poly(ethylene oxide) (PEO) arms, (PSTFSILi)<sub>n</sub>(PEO)<sub>m</sub>, where  $n \approx 22$ , attached to a poly(divinylbenzene) (PDVB) cross-linked core (Figure 9b). These macromolecules behave as core–shell nanoparticles, with PSTFSILi/PEO-rich cores and long PEO arms forming the conductive shell. By varying PSTFSILi arm length, the Li<sup>+</sup>/EO ratio ( $r = 0.046–0.171$ ) was systematically tuned, revealing a clear trade-off: conductivity decreased with increasing PSTFSILi fraction (e.g.,  $\sigma \approx 3 \times 10^{-8} \text{ S cm}^{-1}$  at 30 °C for  $r = 0.046$  vs.  $\approx 1 \times 10^{-7} \text{ S cm}^{-1}$  for linear PSTFSILi-*b*-PEO), but mechanical robustness increased dramatically. Rheological tests at 30 °C showed solid-like, glassy behavior ( $G' \gg G''$ ) for all compositions, with shear modulus rising to  $\approx 1 \text{ GPa}$  at  $\Phi_{\text{PSTFSILi}} = 0.42$ , several orders of magnitude higher than linear block copolymer analogues. Thus, while conductivity is slightly lower than in PSTFSILi-*b*-PEO systems, as the authors compare, the miktoarm architecture delivers exceptionally robust, glass-like electrolytes, highlighting how molecular topology can be leveraged to design single-ion conductors with mechanical integrity sufficient for dendrite suppression.

**Table 2.** Overall characteristics and remarks for non-linear SIPEs, that focus on mechanical integrity.

Reference No.	Preparation Method	Macromolecular architecture	Matrix	Lithium transference number, $t_{\text{Li}^+}$	Mechanical performance	Ionic conductivity ( $\text{S cm}^{-1}$ )	Remarks
63	Emulsion polymerization	Polymeric nanoparticles	LiTFSI/PEO or PC	0.8	$10 - 10^6 \text{ Pa}$ (Storage moduli, rt)	$9.5 \times 10^{-5}$ (20°C) – $2.8 \times 10^{-4}$ (85°C)	Nanoparticles as additives to reinforce modulus
56, 64	NMP polymerization “arm-first”, “in-out”	Miktoarm stars	-	-	$0.01 - 1 \text{ GPa}$ (Storage moduli, 30 °C)	$10^{-8}$ (rt) – $10^{-5}$ (90 °C)	Star architecture dramatically increases mechanical performance over a slight loss of conductivity when compared to linear systems.



### 3.3 Toward Adaptive Functionality: Flexible and Processable Systems

View Article Online  
DOI: 10.1039/D6TA01035K

While progress has been made in improving the electrochemical stability, interfacial compatibility, and mechanical strength of polymer electrolytes, their practical use also depends on processability. Flexibility, thermal shaping, and compatibility with advanced manufacturing methods such as 3D printing are key for real-world integration. The following examples illustrate systems where adaptive functionality and processing ease are central to the design (Figure 10, Table 3).

Cao et al.<sup>65</sup> presented a versatile molecular-level design of intrinsically stretchable single-ion conducting polymer electrolytes (SICPEs), targeting applications in stretchable devices. The networks were synthesized by grafting poly(styrene sulfonyl trifluoromethanesulfonylimide lithium) (STF-Li<sup>+</sup>) or methacrylate-based sulfonylimide monomers (MPA-Li<sup>+</sup>/Na<sup>+</sup>) together with PEGMA side chains onto a PDMS backbone, followed by crosslinking with PDMS segments (Figure 10a). This approach suppressed PEG crystallization, avoided phase separation, and yielded free-standing elastic membranes with tunable crosslinking densities. The membranes exhibited low glass transitions (−19 to −32 °C with PEGMA incorporation, vs. 68.5 °C without), tensile strength between 0.09–0.73 MPa, and elongation at break from 80% up to 252%. Interestingly, while modulus and toughness increased with crosslink density, extensibility showed no clear correlation, attributed to the dual effect of PDMS crosslinking: restricting chain mobility but simultaneously lowering  $T_g$  and shortening relaxation times. Ionic conductivities reached 10<sup>−8</sup>–10<sup>−7</sup> S cm<sup>−1</sup> at room temperature, with faster ionic than segmental dynamics (decoupling behavior). A high lithium transference number ( $t_{Li^+} = 0.79$ ) was measured and assembled Li|SICPE|LFP cells showed stable cycling with 81.5% capacity retention after 100 cycles.

Beyond stretchability, other approaches emphasized quasi-solid designs that combine flexibility with high conductivity for wearable energy storage. Cai et al.<sup>66</sup> designed a series of quasi-solid single-ion polymer electrolytes (PU-TFMSI) with intrinsic flexibility and high ionic conductivity, targeting applications in flexible and wearable Li-metal batteries. The crosslinked networks integrate three complementary segments: (i) Li-rich sulfonimide pendants to provide high ionic conductivity, (ii) soft polyether blocks (PPG-PEG-PPG) to enable chain mobility and stretchability, and (iii) hard polyurethane segments to ensure mechanical stability. 2-hydroxyethyl- $\beta$ -cyclodextrin (HE- $\beta$ -CD) was additionally used to serve as a hyperbranched and crosslinked center (Figure 10b). This molecular design afforded tunable mechanics, with fracture strain ranging from 10% to 1870% and fracture stress from 6.20 to 0.54 MPa, while the optimal composition (PU-TFMSI-2) combined high stretchability (1350%) with toughness



of  $13.6 \text{ MJ m}^{-3}$ . Importantly, the networks remained amorphous (no detectable  $T_g$ ) and thermally stable up to  $300 \text{ }^\circ\text{C}$ . Upon swelling with GBL/FEC, ionic conductivity was significantly enhanced, reaching  $2.65 \times 10^{-4} \text{ S cm}^{-1}$  at  $25 \text{ }^\circ\text{C}$  and up to  $10^{-3} \text{ S cm}^{-1}$  at  $75 \text{ }^\circ\text{C}$ , while  $\text{Li}^+$  transference numbers remained high ( $t_{\text{Li}^+} = 0.87\text{--}0.92$ ). Electrochemical stability extended to  $5.0 \text{ V vs. Li/Li}^+$ , and the optimized PU-TFMSI-2 electrolyte enabled stable Li plating/stripping and uniform SEI formation. In full cells, LFP/PU-TFMSI-2/Li exhibited excellent cycling stability with 99.6% Coulombic efficiency and reliable rate capability, while soft pouch cells maintained performance under bending, demonstrating practical flexibility for wearable applications.

Whereas these systems prioritized stretchability and flexibility, later studies introduced adaptive, self-healing functions to extend membrane lifetime and recyclability. Lee et al.<sup>67</sup> introduced thermally reprocessable and self-healing single-ion polymer electrolytes based on sulfonylimide anionic monomers and thermo-reversible Diels–Alder crosslinking. Linear copolymers of lithium 4-styrenesulfonyl(trifluoromethylsulfonyl)imide (STFSILi) with furfuryl methacrylate (FMA) or furan-terminated poly(ethylene glycol) methacrylate (PEGFMA) were synthesized and subsequently crosslinked with bismaleimide to afford dynamic covalent networks (xLs: STFSILi–FMA; xLPs: STFSILi–PEGFMA, Figure 10c). The thermomechanical properties depended strongly on the electrolyte ratio and comonomer type: higher STFSILi content raised  $T_g$  and reduced mobility, whereas PEGFMA incorporation lowered  $T_g$  and activation energies for relaxation, enabling faster reversible DA exchange. Storage moduli reached  $10^6\text{--}10^8 \text{ Pa}$  in the  $-20$  to  $60 \text{ }^\circ\text{C}$  window, ensuring sufficient rigidity to suppress dendrite growth under battery operating conditions. Interestingly, unlike conventional cross-linked polymers that maintain constant modulus in the rubbery plateau, these materials showed a modulus drop above  $\sim 100 \text{ }^\circ\text{C}$ , attributed to the retro-Diels–Alder dissociation of dynamic crosslinks. This dynamic behavior also meant that increasing the number of crosslinking moieties made the networks more elastic, balancing toughness with reprocessability. Electrochemical characterization showed ionic conductivities of  $\sim 10^{-5}\text{--}10^{-4} \text{ S cm}^{-1}$  between  $40\text{--}80 \text{ }^\circ\text{C}$ , with xLP3 achieving  $7.1 \times 10^{-5} \text{ S cm}^{-1}$  at  $80 \text{ }^\circ\text{C}$ . All samples exhibited high lithium transference numbers ( $t_{\text{Li}^+} > 0.75$ ) and wide electrochemical stability windows ( $4.6\text{--}5.6 \text{ V}$ ). Importantly, the materials demonstrated full self-healing at  $140 \text{ }^\circ\text{C}$  and retained mechanical and ionic properties over 30 reprocessing cycles, highlighting their promise as recyclable, safe solid polymer electrolytes.

Apart from thermo-reversible self-healing mechanisms, supramolecular strategies offered an alternative route to enable reprocessability and adaptive recovery of properties. Gan et al.<sup>68</sup>



designed self-healing single-ion polymer electrolytes (SIPEs) by copolymerizing poly(ethylene glycol) methacrylate (PEGMA), styrene sulfonyl(trifluoromethanesulfonyl)imide lithium (SSPSILi), and ureidopyrimidinone methacrylate (UPyMA) through RAFT polymerization, followed by solvent casting into free-standing membranes (Figure 10d). Each component played a distinct role: PEGMA side chains promoted ion mobility and flexibility, SSPSILi units immobilized anions and provided mechanical reinforcement, while UPy groups introduced dynamic supramolecular hydrogen bonding that enabled reprocessability and self-healing. The copolymers were amorphous, with low glass transitions ( $-49$  to  $-16$  °C) and good thermal stability up to  $250$  °C. Mechanical testing showed tensile stresses of  $0.045$ – $0.739$  MPa and elongations of  $99$ – $427\%$ , with SIPE-5 achieving  $\sim 0.51$  MPa and  $288\%$  strain. Ionic conductivity ranged from  $1.9 \times 10^{-6}$  to  $1.9 \times 10^{-5}$  S·cm $^{-1}$  at  $60$  °C, while the lithium transference number remained high ( $t_{Li^+} = 0.89$ ). In Li|Li symmetric cells, the incorporation of SSPSILi was critical for interfacial stability, as SIPE-5 operated stably for  $2800$  h of Li stripping/plating without short-circuit or dendrite formation, in contrast to systems lacking SSPSILi. Notably, damaged membranes could be fully restored by thermal annealing, recovering both mechanical integrity and conductivity, underscoring the potential of supramolecular hydrogen bonding as a robust strategy for safe, recyclable SPEs.

Building on these advances in adaptive membranes, the next systems leveraged nanoparticle design and tailored plasticization to achieve not only flexibility but also direct printability. Gallastegui et al.<sup>69</sup> reported methacrylate-based single-ion polymer nanoparticles (LiPNPs) synthesized via emulsion copolymerization of methyl methacrylate and LiMTFSI methacrylate (Figure 10e), yielding small particles ( $22$ – $30$  nm) with high surface density of sulfonamide lithium groups. These LiPNPs were incorporated into gel polymer electrolytes with carbonate or sulfolane plasticizers, producing conductivities between  $2.9 \times 10^{-4}$  and  $2.3 \times 10^{-5}$  S cm $^{-1}$  at  $85$  °C, with the best performance achieved for smaller NPs of higher Li content. Compared to their earlier system employing  $\sim 100$  nm particles<sup>63</sup>, the finer dispersion provided  $\sim 3\times$  higher conductivity at equal conditions, attributed to the increased surface exposure of tethered anions to the mobile phase. In general, ionic conductivity was enhanced by the addition of Li ions (over the  $25$ – $85$  °C range), thus favoring the gel electrolytes containing NPs with higher Li content. This tendency is also reflected in the storage modulus, where the authors hypothesize that higher lithium concentration generates a solvation shell through interaction with the plasticizer, thereby increasing the softness of the gel. Notably, sulfolane-based gels formed malleable, extrusion-printable inks, enabling layer-by-layer fabrication of polymer electrolytes by direct ink writing (DIW). These printed membranes exhibited room-temperature



conductivities up to  $1.7 \times 10^{-5} \text{ S cm}^{-1}$ , a lithium transference number of 0.67, and stable cycling in Li|Li symmetric cells. This study underscores how nanoscale design and tailored plasticization can enable polymer electrolytes that combine high ionic conductivity with extrusion printability and processing versatility.

More recently, additional comonomer engineering expanded this nanoparticle-based approach, revealing how subtle structural changes alter the balance of conductivity, mechanics, and stability. Herranz Berzosa et al.<sup>70</sup> expanded the single-ion nanoparticle approach by introducing additional comonomers into MTFSiLi–MMA nanoparticles, synthesizing three families: poly(MTFSiLi-*co*-MMA) NPs, poly(MTFSiLi-*co*-MMA-*co*-Sty) NPs, and poly(MTFSiLi-*co*-MMA-*co*-PEGMA) NPs (Figure 10f). The pristine nanoparticles (20–30 nm) showed distinct glass transitions depending on composition: 110 °C (MMA), 127 °C (Sty-containing), and 101 °C (PEGMA-containing). When blended with sulfolane (50 wt%) to form quasi-solid SIPEs, the mixtures displayed dramatically reduced glass transition temperatures of –61 °C (MMA) and –54 °C (PEGMA), while no  $T_g$  was observed within –75 to 100 °C for the Sty-based sample, reflecting stronger polymer–plasticizer interactions. Electrochemically, styrene incorporation imparted stiffer membranes but reduced conductivity ( $1 \times 10^{-5} \text{ S cm}^{-1}$  at 95 °C). Conversely, PEGMA lowered the  $T_g$  and increased chain dynamics, yet conductivity did not improve as expected when compared to the MMA-only system, which reached  $3 \times 10^{-4} \text{ S cm}^{-1}$  at 95 °C. This softening also compromised long-term stability: the PEGMA-based SIPE short-circuited after ~200 h in Li|Li cells, whereas the styrene system maintained longer stability (albeit with slightly higher overpotential). The MMA-only reference, by contrast, showed higher conductivity but poor interfacial compatibility, rapidly polarizing in symmetric cells. Transference numbers mirrored these trends, with the styrene-based SIPE yielding the highest value (0.69) versus 0.57 for MMA and PEGMA systems. Altogether, this comparative study underscores how modest comonomer changes reshape  $T_g$ , ion transport, and stability, highlighting the molecular trade-offs between rigidity, mobility, and interfacial robustness in quasi-solid SIPEs.

View Article Online  
DOI: 10.1039/D6TA01035K



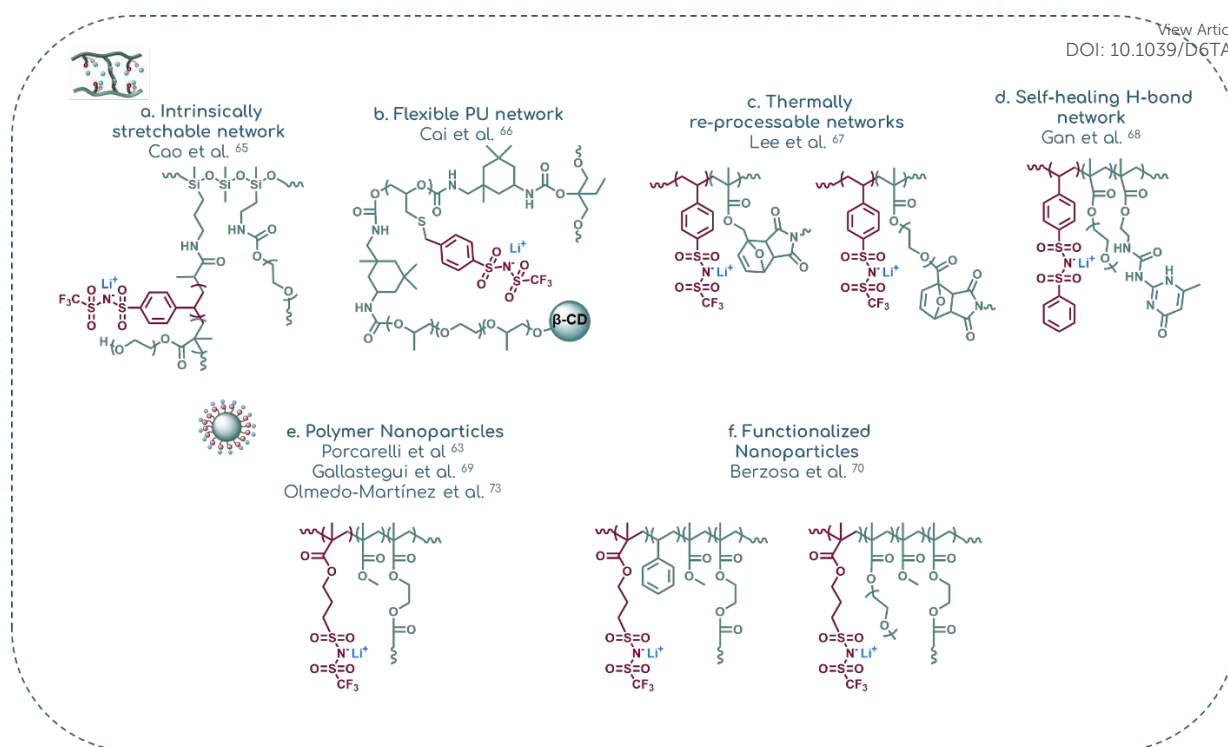


**Figure 11.** Chemical structures and the associated macromolecular architectures, for SIPE systems prioritizing flexibility and/or reprocessability. The representative architecture of each system is shown above its corresponding chemical structure, while the red-highlighted moieties identify the ion-bearing groups and the green-highlighted segments indicate the rest of the polymer structure.



**Table 3.** Overall characteristics and remarks for non-linear SIPEs, that focus on Flexible and/or Processable Systems.

View Article Online

DOI: 10.1039/D0TA01035K

Reference No.	Preparation Method	Macromolecular architecture	Matrix	Lithium transference number, $t_{Li^+}$	Mechanical performance	Ionic conductivity ( $S\ cm^{-1}$ )	Remarks
65	RAFT polymerization, cross-linking	Network of branches	-	0.79	0.09 – 0.73 MPa (Tensile strength) Elongation at break: 88 – 252%	$10^{-8}$ – $10^{-7}$ (rt)	Inherently stretchable SICPE networks
66	Polycondensation, cross-linking	PU network	GBL/FEC plasticizer	0.87-0.92	10 – 1870 % fracture stress	$1.31 – 2.65 \times 10^{-4}$ (rt)	PU-segmented, stretchable quasi-solid SIPEs; high toughness, conductivity, and pouch-cell flexibility
67	Radical polymerization and thermoreversible cross-linking	Thermoreversible crosslinked networks	-	0.75-0.93	Storage modulus: $10^6$ – $10^8$ Pa (–20 to 60 °C range). Tensile strength: up to ~3 MPa. Elongation at break: 5–20%	$7.8 \times 10^{-6}$ (40 °C)– $7.1 \times 10^{-5}$ (80 °C)	Self-healing recyclable networks
68	RAFT polymerization	Linear copolymer supramolecular networks	-	0.89	Stress: 0.045 – 0.739 MPa Strain: 99–427%	$1.88 \times 10^{-6}$ – $1.86 \times 10^{-5}$ (60 °C)	Self-healing via supramolecular H-bonds
69	Emulsion polymerization	Polymeric nanoparticles	Sulfolane or DMC/FC	0.67	$10^5 – 10^6$ Pa (Storage moduli, 50 °C)	$2.3 \times 10^{-5}$ – $2.9 \times 10^{-4}$ (85 °C)	Printable SIPE – nanoparticle gels
70	Emulsion polymerization	Polymeric nanoparticles	Sulfolane	0.57-0.69	-	$10^{-6}$ – $10^{-5}$ (approx. - rt), $10^{-4}$ (approx. - 95 °C)	Quasi-solid SIPES stability vs. mobility



### 3.4 Multifunctional Systems Bridging Performance Domains

View Article Online  
DOI: 10.1039/D6TA01035K

The development of solid polymer electrolytes is often driven by the optimization of a single property, such as conductivity, toughness, or processability. Yet these characteristics are rarely independent, and improvements in one domain frequently compromise another. In response, recent research has explored multifunctional polymer designs that aim to balance, or even decouple, these antagonistic effects. Through careful molecular and network design, these systems demonstrate how mechanical integrity, electrochemical performance, and adaptive features can coexist within a single material platform. The following studies exemplify such unified approaches, where multifunctionality emerges as a guiding principle rather than an afterthought (Figure 11, Table 4).

Building directly on their previous work on miktoarm star SPEs<sup>54,62</sup>, Nikolakakou et al.<sup>71,72</sup> designed nanostructured single-ion polymer blend electrolytes by blending core-shell polyanionic particles, composed of asymmetric miktoarm stars with poly(styrene-4-sulfonyltrifluoromethylsulfonyl)imide lithium (PSTFSILi) arms complementing longer poly(ethylene oxide) (PEO) arms (Figure 9a), into low molecular weight PEO (PEG-0.5K). The PEG matrix acts simultaneously as a plasticizer and ion-conducting phase, promoting miscibility and interconnected transport channels, while the star copolymers supply immobilized anions and mechanical reinforcement. Remarkably, for loadings  $\leq 55$  wt%, the blends form nanostructured electrolytes with continuous PEG-rich channels, where  $\text{Li}^+$  conductivity decreases only slightly across compositions (from  $5.0 \times 10^{-6}$  to  $3.1 \times 10^{-6}$  S  $\text{cm}^{-1}$  at 30 °C for 30–55 wt% blends), while the shear modulus increases by more than three orders of magnitude with increasing particle loading. This demonstrates a strong decoupling between ionic conductivity and mechanical performance. By contrast, at higher loadings (>55 wt%), overlapping of the star particles disrupts PEG connectivity, shifting ion transport from diffusion-dominated to hopping-dominated pathways and causing conductivity deterioration. Still, when compared to the liquid PEG-0.5K/LiTFSI electrolyte, the 55 wt% blend exhibits a shear modulus more than five orders of magnitude higher, while the  $\text{Li}^+$  conductivity is less than one order of magnitude lower, highlighting the exceptional balance achieved in this system.

Extending this “all-polymer” concept, Olmedo-Martínez et al.<sup>73</sup> reported salt-free polymer nanocomposites composed of lithium sulfonamide-functionalized PMMA nanoparticles (LiNPs, ~25 nm, Figure 10e) uniformly dispersed within a PEO matrix. The small size and high surface functionality of the LiNPs reduced the crystallinity of PEO (completely suppressed at 70 wt% LiNPs), thereby enhancing the amorphous content available for ion transport. Ionic



conductivity was evaluated across several compositions (15–70 wt%) and temperatures (40–90 °C), showing high values at elevated temperatures ( $10^{-6}$ – $10^{-5}$  S cm<sup>-1</sup> at 90 °C), but steep crystallization-induced drops at low particle contents (15–30 wt%) and rigidity-limited performance at very high contents (70 wt%). As a result, the 50 wt% LiNPs composite was identified as the optimal balance, maintaining conductivity over a broad temperature range while avoiding crystallization effects. This sample delivered a lithium transference number of 0.68, a storage modulus of  $\sim 10^8$  Pa above PEO's melting transition, and stable Li||Li cycling for over 1000 h without dendritic failure. Furthermore, a full Li|PEO-LiNPs|LFP cell achieved  $\sim 150$  mAh g<sup>-1</sup> at C/10 (0.05 mA cm<sup>-2</sup>, 3.8–2.8 V). This work demonstrates a compelling multifunctional balance, where ionic conductivity, lithium-ion selectivity, and mechanical reinforcement are simultaneously achieved in a salt-free solid-state system.

Transitioning from particle–matrix blends to fiber-supported membranes, Zhang et al.<sup>74</sup> synthesized a crosslinked single-ion polymer electrolyte (SIGPE) using a UV-initiated thiol-ene click reaction of lithium (4-styrenesulfonyl)(trifluoromethanesulfonyl) imide (STFSILi), pentaerythritol tetrakis(2-mercaptoacetate) (PTMP), and pentaerythritol tetraacrylate (PETA) within a polypropylene (PP) nonwoven fabric (Figure 11a). After swelling with EC/DMC solvent, the resulting gel exhibited high ionic conductivity (0.84 mS cm<sup>-1</sup> at 25 °C, 1.76 mS cm<sup>-1</sup> at 80 °C), a Li<sup>+</sup> transference number of 0.93, and a wide electrochemical window of 5.2 V vs. Li<sup>+</sup>/Li. While mechanical strength decreased upon swelling (tensile strength from 3.8 to 2.8 MPa), the membrane remained robust enough to function as both electrolyte and separator. In LiFePO<sub>4</sub>||Li cells, the electrolyte delivered long-term stability with 83% capacity retention after 400 cycles at 1C and nearly 100% coulombic efficiency. This work illustrates how thiol-ene click chemistry enables multifunctional balance by combining ionic conductivity, selectivity, stability, and sufficient mechanics in a practical, processable design.

Cheng et al.<sup>75</sup> who developed polyacrylonitrile (PAN) nanofiber-reinforced SIPE membranes via UV-initiated polymerization of STFSILi and PEGDA in the presence of propylene carbonate (PC) as plasticizer (0.5–2.5 weight ratio to dry SIPE, Figure 11b). While the plasticized network (SIPE-2.5) reached high ionic conductivity ( $1.18 \times 10^{-3}$  S cm<sup>-1</sup> at 25 °C) and a lithium transference number of 0.93, its weak mechanical performance (0.76 MPa modulus, 0.03 MPa tensile strength, 2.6% elongation) limited applicability. Reinforcement with electrospun PAN nanofibers (SIPE-2.5-PAN) preserved high conductivity ( $8.09 \times 10^{-4}$  S cm<sup>-1</sup>), while dramatically boosting mechanics (5.91 MPa modulus, 4.45 MPa tensile strength, 152% elongation) and extending the electrochemical window to 4.9 V. In terms of thermal stability, SIPE-2.5-PAN remained stable up to  $\sim 100$  °C but exhibited PC volatilization above this range,



whereas the dry SIPE and PAN nanofibers were independently stable above 300–350 °C. A low activation energy of 0.19 eV confirmed facile ion transport, while electrochemical testing showed long-term Li||Li stability (>1000 h without dendritic failure) and excellent Li|LFP cycling. This system stands out as a clear example of multifunctional balance achieved through plasticization–reinforcement synergy.

Using a different approach to achieve mechanical robustness, Zhou et al.<sup>76</sup> demonstrated how hierarchical brush topologies can deliver both stiffness and transport. They designed ultrathin bottlebrush electrolytes by grafting poly(lithium 4-styrenesulfonyl(trifluoromethylsulfonyl)imide)-*b*-poly(diethylene glycol monomethyl ether methacrylate) (PSTFSILi-*b*-PEGM) diblocks from bacterial cellulose (BC) nanofibrils (Figure 11c). The resulting porous nanonetworks combined a rigid BC backbone with mobile side chains, yielding free-standing membranes with high mechanical strength (2.2 GPa) and ionic conductivity of  $4.9 \times 10^{-6} \text{ S cm}^{-1}$  at room temperature. Incorporation of 25 wt% plasticizer (BC-*g*-PSTFSILi-*b*-PEGM/P) further enhanced conductivity to  $3.1 \times 10^{-4} \text{ S cm}^{-1}$  while maintaining high modulus (1.9 GPa). Importantly, the BC-*g*-PSTFSILi-*b*-PEGM/P system also exhibited a high lithium transference number ( $t_{\text{Li}^+} = 0.85$ ). The molecular design proved critical for interfacial stability: while simpler systems (BC alone, BC-*b*-PEGM, or BC-*g*-PSTFSILi without the PEGM block) showed rapid failure with high overpotentials ( $\approx 73$ –150 mV) and short circuits within 100–150 h, the full BC-*g*-PSTFSILi-*b*-PEGM/P brush system maintained stable cycling for over 3300 h in Li||Li cells with an overpotential of 5 mV. The dual block architecture reduced interfacial resistance, ensured good adhesion to Li metal, and effectively suppressed dendrite growth. This work highlights how careful integration of hard, soft, and ion-conducting segments in a hierarchical brush topology enables a unique balance of mechanical robustness, ionic selectivity, and long-term electrochemical stability.

Finally, to generalize design approaches for crosslinked systems, Shen et al.<sup>77</sup> reported a model system of single-ion conducting networks with an acrylate backbone, ethylene oxide (EO) side chains, tethered fluorinated anions, and mobile Li<sup>+</sup> cations, designed to map out structure–property relationships (Figure 11d). By systematically varying four parameters: crosslinker content, crosslinker length, Li:EO ratio, and EO side-chain length, the authors disentangled how each molecular feature impacts conductivity,  $T_g$ , and modulus. At low crosslinking density (<8 mol%), the modulus could be increased by a factor of 8 (up to 2.4 MPa) without loss of conductivity, providing a design principle for dendrite-suppressing electrolytes. A maximum in conductivity was observed at room temperature around a Li:EO ratio of 1:40, reflecting the balance between ion concentration and segmental mobility, while at elevated temperatures



conductivity increased monotonically with Li content. Extending side-chain length from 3 to 6 EO units substantially enhanced conductivity, even after normalizing for  $T_g$ , emphasizing that subtle chemical modifications strongly affect solvation and ion transport. Overall, conductivity varied by two orders of magnitude at 90 °C and three at room temperature, depending on molecular details. The best-performing networks reached  $\sim 10^{-5}$  S  $\text{cm}^{-1}$  at high temperature, and incorporation of 10 wt% propylene carbonate (PC) further boosted this value to  $10^{-4}$  S  $\text{cm}^{-1}$  while retaining single-ion character ( $t_{\text{Li}} \approx 0.85$ ). This work provides fundamental insight into how molecular design governs decoupling of ionic and mechanical properties in network polymer electrolytes.

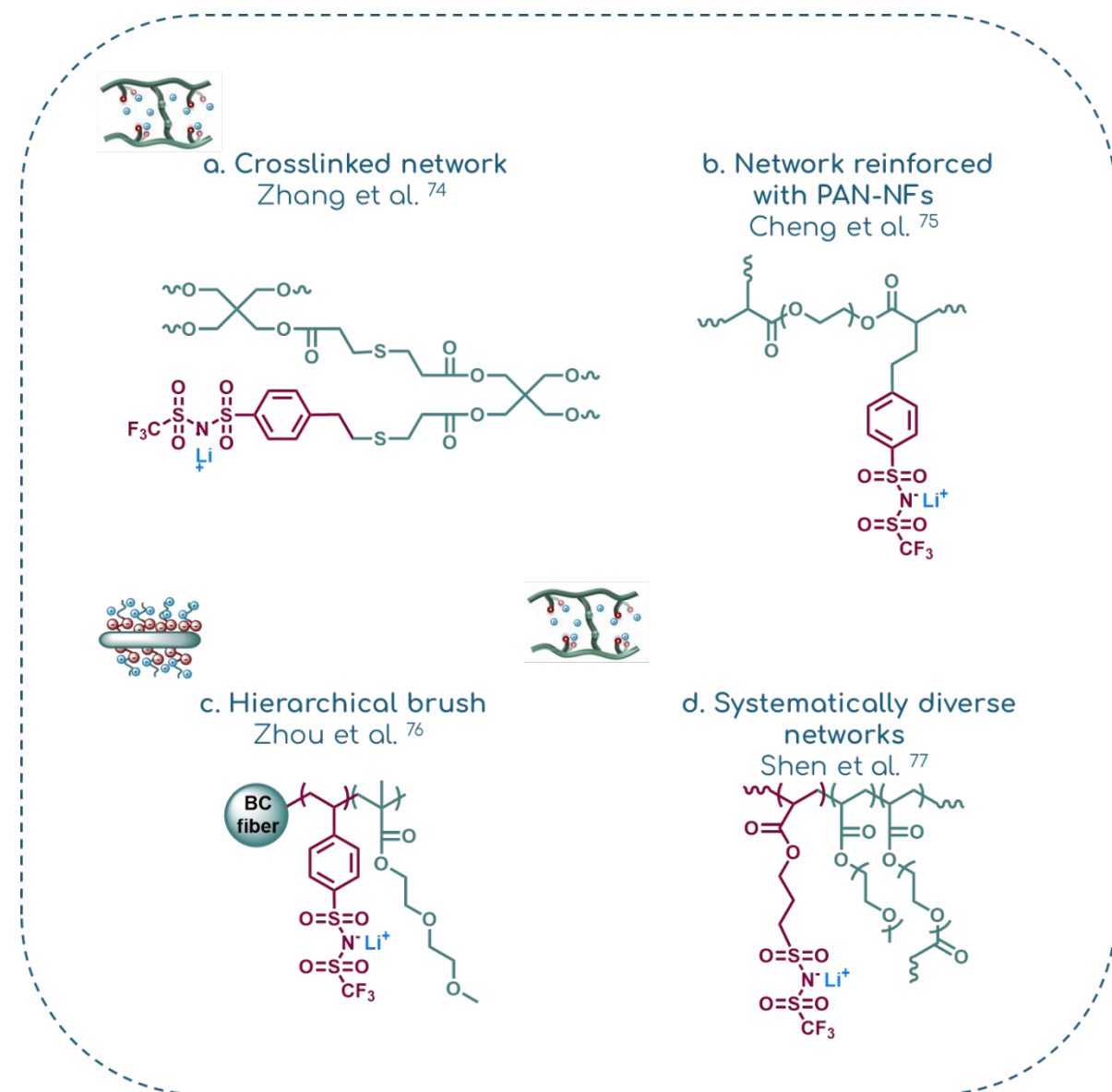


**Figure 12.** Chemical structures and the associated macromolecular architectures, for SIPE systems prioritizing diverse functionalities. The representative architecture of each system is shown above its corresponding chemical structure; the red-highlighted moieties indicate the



ion-bearing groups, whereas the green-highlighted segments correspond to the remaining polymer structure.

**Table 4** Overall characteristics and remarks for non-linear SIPEs, that focus on multifunctional performance.

Reference Number	Method of preparation	Macromolecular architecture	Matrix	Lithium transference number, $t_{Li^+}$	Mechanical performance	Ionic conductivity ( $S\ cm^{-1}$ )	Remarks
71	NMP polymerization “arm-first”, “in-out”	Miktoarm stars	PEO 0.5K	-	10 - 10 <sup>7</sup> Pa (Shear moduli, rt)	10 <sup>-7</sup> – 10 <sup>-5</sup> (rt)	Decoupling of conductivity and mechanics
73	Emulsion polymerization	Nanoparticles	PEO 100K	0.68	Approx. 10 <sup>8</sup> Pa (Storage moduli, 80 °C)	10 <sup>-8</sup> – 10 <sup>-6</sup> (40 °C)	Salt-free nanocomposite
74	UV initiated thiol-ene click reaction	Crosslinked network	PP fabric with EC/DMC	0.93	2.8 (swollen) – 3.8 (dry) MPa	8.4 × 10 <sup>-4</sup> (25 °C), 1.76 × 10 <sup>-3</sup> (80 °C)	Synergy of conductivity and stability
75	UV initiated free radical polymerization	Network, reinforced by PAN-NFs	PC plasticizer, PAN nanofibers	0.92	Young's modulus: 5.91 MPa, Tensile strength: 4.45 MPa, Elongation: 152%	8.09 × 10 <sup>-4</sup> (25 °C)	PAN-NF reinforced SIPE. Flexible and highly conductive
76	Surface Initiated ATRP	Bottlebrush porous nanonetwork	Dimethyl ether dioxolane	0.85	Young's modulus: 2.2 GPa (dry), 1.9 GPa (25% plasticizer)	4.9 × 10 <sup>-6</sup> (25 °C), 3.1 × 10 <sup>-4</sup> (25 °C with plasticizer)	Decoupling of conductivity and mechanics. Dendrite suppression



77	UV polymerization	Crosslinked network	Plasticize r up to 10%	0.85	Up to 2.4 MPa	Approx $10^{-5}$ (90 °C) Approx $10^{-4}$ (90 °C with 10% PC)	View Article Online DOI: 10.1039/D6TA01035K Systematic study of structure - properties
----	----------------------	------------------------	------------------------------	------	------------------	---	--



#### 4. Conclusions, Future Outlook and Sustainability Considerations

View Article Online  
DOI: 10.1039/D6TA01035K

In recent years, single-ion polymer electrolytes (SIPEs) have progressed beyond their early, academically centered development and are now entering a stage of accelerated innovation aimed at practical deployment. Advances in molecular design, control over morphology, and integration into diverse architectures, such as host matrices, nanocomposites, and hybrid systems, are enabling SIPEs with improved ionic efficiency, robust electrochemical performance, and tunable mechanical properties. As highlighted throughout this review, both chemical design and macromolecular architecture play a central role in governing structure-property relationships, providing complementary strategies to balance ion transport, mechanical integrity, and electrochemical stability.

Despite these advances, several key scientific challenges remain. Interfacial stability with lithium metal and high-voltage cathodes continues to limit long-term performance, particularly under high current densities and extended cycling conditions. While SIPEs inherently suppress concentration polarization through high lithium transference numbers, the fundamental mechanisms governing lithium dendrite suppression remain incompletely understood and depend on a complex interplay between mechanical modulus, ion flux homogeneity, and interfacial chemistry. In addition, achieving high ionic conductivity at ambient temperature while maintaining sufficient mechanical robustness and processability remains a central trade-off across both linear and non-linear SIPE systems.

Looking ahead, future research is expected to increasingly adopt a more holistic design philosophy that bridges molecular-level control with manufacturing and device requirements. In parallel, sustainability considerations are likely to become a defining priority in SIPE development. Emerging strategies such as fluorine-free anion chemistries, including cyano-substituted and dicyano-based systems<sup>21,22</sup> have already demonstrated promising ionic conductivity and improved environmental compatibility compared to conventional fluorinated sulfonylimides. Similarly, the development of bio-based and renewable polymer backbones, such as cellulose-derived architectures<sup>76</sup>, offers a pathway toward more sustainable electrolyte systems while maintaining mechanical robustness. In addition, greener and scalable synthesis approaches, including UV-curing and solvent-free or low-solvent processing routes<sup>58-61</sup>, are gaining increasing attention as viable strategies for reducing environmental impact and facilitating industrial translation.

Beyond materials chemistry, emerging research paradigms are expected to play an increasingly important role in accelerating SIPE development. Machine learning-assisted materials design and high-throughput screening approaches have recently demonstrated strong potential to



capture complex structure–property relationships and guide the discovery of advanced electrolyte materials more efficiently than traditional trial-and-error methods<sup>78</sup>. These approaches are particularly well-suited to SIPE systems, where ion transport depends on a multidimensional parameter space involving polymer chemistry, architecture, and morphology. Coupled with advanced experimental and computational characterization techniques, such data-driven strategies are expected to play a key role in enabling predictive design of next-generation SIPEs.

Ultimately, the continued advancement of SIPEs will depend on the ability to integrate electrochemical performance, mechanical robustness, processability, and sustainability within a unified design framework. By combining rational molecular engineering with scalable fabrication strategies and environmentally responsible materials selection, SIPEs are well-positioned to evolve from model systems into practical components of next-generation energy storage technologies.

### **Author contributions**

M. T. and A. S. wrote the manuscript with the help of the other co-authors. C. P. and G. S. supervised, reviewed and edited the manuscript. All the authors discussed and commented on the manuscript.

### **Conflicts of interest**

There are no conflicts to declare.

### **Data availability**

No data were generated in this work.



**AUTHOR INFORMATION**View Article Online  
DOI: 10.1039/D6TA01035K**Corresponding Author**

Christos Pantazidis – Department of Chemistry, National and Kapodistrian University of Athens, Athens 15784, Greece; orcid.org/0000-0002-1852-2558;

Email: [chpantaz@chem.uoa.gr](mailto:chpantaz@chem.uoa.gr)

Georgios Sakellariou – Department of Chemistry, National and Kapodistrian University of Athens, Athens 15784, Greece; orcid.org/0000-0003-2329-8084;

Email: [gsakellariou@chem.uoa.gr](mailto:gsakellariou@chem.uoa.gr)

**Authors**

Marileta Tsakanika – Department of Chemistry, National and Kapodistrian University of Athens, Athens 15784, Greece; orcid.org/0009-0004-2157-0501.

Anastasia Stergiou – Department of Chemistry, National and Kapodistrian University of Athens, Athens 15784, Greece; orcid.org/0009-0005-3175-4205.



## References

- (1) Global-Energy-Perspective-2025.Pdf.  
<https://www.mckinsey.com/~media/mckinsey/industries/energy%20and%20materials/our%20insights/global%20energy%20perspective%202025/global-energy-perspective-2025.pdf> (accessed 2025-11-17).
- (2) Deng, J.; Bae, C.; Denlinger, A.; Miller, T. Electric Vehicles Batteries: Requirements and Challenges. *Joule* **2020**, *4* (3), 511–515. <https://doi.org/10.1016/j.joule.2020.01.013>.
- (3) Long, L.; Wang, S.; Xiao, M.; Meng, Y. Polymer Electrolytes for Lithium Polymer Batteries. *J. Mater. Chem. A* **2016**, *4* (26), 10038–10069. <https://doi.org/10.1039/C6TA02621D>.
- (4) Ngai, K. S.; Ramesh, S.; Ramesh, K.; Juan, J. C. A Review of Polymer Electrolytes: Fundamental, Approaches and Applications. *Ionics* **2016**, *22* (8), 1259–1279. <https://doi.org/10.1007/s11581-016-1756-4>.
- (5) Mecerreyes, D.; Casado, N.; Villaluenga, I.; Forsyth, M. Current Trends and Perspectives of Polymers in Batteries. *Macromolecules* **2024**, *57* (7), 3013–3025. <https://doi.org/10.1021/acs.macromol.3c01971>.
- (6) Xue, Z.; He, D.; Xie, X. Poly(Ethylene Oxide)-Based Electrolytes for Lithium-Ion Batteries. *J. Mater. Chem. A* **2015**, *3* (38), 19218–19253. <https://doi.org/10.1039/C5TA03471J>.
- (7) S, R. P.; Prasannavenkadesan, V.; Katiyar, V.; Achalkumar, A. S. Polymer Electrolytes: Evolution, Challenges, and Future Directions for Lithium-Ion Batteries. *RSC Appl. Polym.* **2025**, *3* (3), 499–531. <https://doi.org/10.1039/D4LP00325J>.
- (8) Meng, N.; Ye, Y.; Yang, Z.; Li, H.; Lian, F. Developing Single-Ion Conductive Polymer Electrolytes for High-Energy-Density Solid State Batteries. *Adv. Funct. Mater.* **2023**, *33* (43), 2305072. <https://doi.org/10.1002/adfm.202305072>.
- (9) Zhang, H.; Li, C.; Piszcz, M.; Coya, E.; Rojo, T.; Rodriguez-Martinez, L. M.; Armand, M.; Zhou, Z. Single Lithium-Ion Conducting Solid Polymer Electrolytes: Advances and Perspectives. *Chem. Soc. Rev.* **2017**, *46* (3), 797–815. <https://doi.org/10.1039/C6CS00491A>.
- (10) Zhu, J.; Zhang, Z.; Zhao, S.; Westover, A. S.; Belharouak, I.; Cao, P.-F. Single-Ion Conducting Polymer Electrolytes for Solid-State Lithium–Metal Batteries: Design, Performance, and Challenges. *Adv. Energy Mater.* **2021**, *11* (14), 2003836. <https://doi.org/10.1002/aenm.202003836>.
- (11) Glynos, E.; Pantazidis, C.; Sakellariou, G. Designing All-Polymer Nanostructured Solid Electrolytes: Advances and Prospects. *ACS Omega* **2020**, *5* (6), 2531–2540. <https://doi.org/10.1021/acsomega.9b04098>.
- (12) Diederichsen, K. M.; McShane, E. J.; McCloskey, B. D. Promising Routes to a High Li<sup>+</sup> Transference Number Electrolyte for Lithium Ion Batteries. *ACS Energy Lett.* **2017**, *2* (11), 2563–2575. <https://doi.org/10.1021/acsenergylett.7b00792>.
- (13) Sahu, A. K.; Varadwaj, K. S. K.; Nayak, S. K.; Mohanty, S. Single-Ion Conducting Polymer Electrolyte: A Promising Electrolyte Formulation to Extend the Lifespans of LMBs. *Nano Energy* **2024**, *122*, 109261. <https://doi.org/10.1016/j.nanoen.2024.109261>.
- (14) Gao, J.; Wang, C.; Han, D.-W.; Shin, D.-M. Single-Ion Conducting Polymer Electrolytes as a Key Jigsaw Piece for next-Generation Battery Applications. *Chem. Sci.* **2021**, *12* (40), 13248–13272. <https://doi.org/10.1039/D1SC04023E>.
- (15) Bocharova, V.; Sokolov, A. P. Perspectives for Polymer Electrolytes: A View from Fundamentals of Ionic Conductivity. *Macromolecules* **2020**, *53* (11), 4141–4157. <https://doi.org/10.1021/acs.macromol.9b02742>.



- (16) An, Y.; Han, X.; Liu, Y.; Azhar, A.; Na, J.; Nanjundan, A. K.; Wang, S.; Yu, J.; Yamachi, Y. Progress in Solid Polymer Electrolytes for Lithium-Ion Batteries and Beyond. *ACS Appl. Mater. Interfaces* **2022**, *14* (16), 18324–18334. <https://doi.org/10.1021/acsami.1c25067>. View Article Online  
DOI: 10.1039/D6PA01035K
- (17) Ghorbanzade, P.; Loaiza, L. C.; Johansson, P. Plasticized and Salt-Doped Single-Ion Conducting Polymer Electrolytes for Lithium Batteries. *RSC Adv.* **2022**, *12* (28), 18164–18167. <https://doi.org/10.1039/D2RA03249J>.
- (18) Kondou, S.; Sakashita, Y.; Yang, X.; Hashimoto, K.; Dokko, K.; Watanabe, M.; Ueno, K. Li-Ion Transport and Solvation of a Li Salt of Weakly Coordinating Polyanions in Ethylene Carbonate/Dimethyl Carbonate Mixtures. *ACS Appl. Mater. Interfaces* **2022**, *14* (16), 18324–18334. <https://doi.org/10.1021/acsami.1c25067>.
- (19) Zhao, S.; Song, S.; Wang, Y.; Keum, J.; Zhu, J.; He, Y.; Sokolov, A. P.; Cao, P.-F. Unraveling the Role of Neutral Units for Single-Ion Conducting Polymer Electrolytes. *ACS Appl. Mater. Interfaces* **2021**, *13* (43), 51525–51534. <https://doi.org/10.1021/acsami.1c15641>.
- (20) Shao, Z.; Nederstedt, H.; Jannasch, P. Styrenic BAB Triblock Copolymers Functionalized with Lithium (N-Tetrafluorophenyl)Trifluoromethanesulfonamide as Solid Single-Ion Conducting Electrolytes. *ACS Appl. Energy Mater.* **2021**, *4* (3), 2570–2577. <https://doi.org/10.1021/acsaem.0c03141>.
- (21) Yuan, H.; Luan, J.; Yang, Z.; Zhang, J.; Wu, Y.; Lu, Z.; Liu, H. Single Lithium-Ion Conducting Solid Polymer Electrolyte with Superior Electrochemical Stability and Interfacial Compatibility for Solid-State Lithium Metal Batteries. *ACS Appl. Mater. Interfaces* **2020**, *12* (6), 7249–7256. <https://doi.org/10.1021/acsami.9b20436>.
- (22) Martinez-Ibañez, M.; Sanchez-Diez, E.; Qiao, L.; Meabe, L.; Santiago, A.; Zhu, H.; O'Dell, L. A.; Carrasco, J.; Forsyth, M.; Armand, M.; Zhang, H. Weakly Coordinating Fluorine-Free Polysalt for Single Lithium-Ion Conductive Solid Polymer Electrolytes. *Batter. Supercaps* **2020**, *3* (8), 738–746. <https://doi.org/10.1002/batt.202000045>.
- (23) Liu, J.; Schaefer, J. L. Li<sup>+</sup> Conduction in Glass-Forming Single-Ion Conducting Polymer Electrolytes with and without Ion Clusters. *Macromolecules* **2023**, *56* (6), 2515–2525. <https://doi.org/10.1021/acs.macromol.2c02516>.
- (24) Mei, W.; Yu, D.; George, C.; Madsen, L. A.; Hickey, R. J.; Colby, R. H. Anion Chemical Composition of Poly(Ethylene Oxide)-Based Sulfonylimide and Sulfonate Lithium Ionomers Controls Ion Aggregation and Conduction. *J. Mater. Chem. C* **2022**, *10* (39), 14569–14579. <https://doi.org/10.1039/D2TC02212E>.
- (25) Kadulkar, S.; Brotherton, Z. W.; Lynch, A. L.; Pohlman, G.; Zhang, Z.; Torres, R.; Manthiram, A.; Lynd, N. A.; Truskett, T. M.; Ganesan, V. The Importance of Morphology on Ion Transport in Single-Ion, Comb-Branched Copolymer Electrolytes: Experiments and Simulations. *Macromolecules* **2023**, *56* (7), 2790–2800. <https://doi.org/10.1021/acs.macromol.2c02500>.
- (26) Yang, M.; Epps, T. H. I. Solid-State, Single-Ion Conducting, Polymer Blend Electrolytes with Enhanced Li<sup>+</sup> Conduction, Electrochemical Stability, and Limiting Current Density. *Chem. Mater.* **2024**, *36* (4), 1855–1869. <https://doi.org/10.1021/acs.chemmater.3c02389>.
- (27) Chouirfa, H.; Gomri, C.; Benkhaled, B. T.; Chaix, A.; Aissou, K.; Semsarilar, M. Single-Ion Nano-Features Formed by a Li-Containing Block Copolymer Synthesized via PISA. *Polym. Chem.* **2023**, *14* (25), 2971–2978. <https://doi.org/10.1039/D3PY00284E>.
- (28) Lozinskaya, E. I.; Ponkratov, D. O.; Malyshkina, I. A.; Grysan, P.; Lingua, G.; Gerbaldi, C.; Shaplov, A. S.; Vygodskii, Y. S. Self-Assembly of Li Single-Ion-Conducting Block Copolymers for Improved Conductivity and Viscoelastic Properties. *Electrochimica Acta* **2022**, *413*, 140126. <https://doi.org/10.1016/j.electacta.2022.140126>.
- (29) Zhang, B.; Zheng, C.; Sims, M. B.; Bates, F. S.; Lodge, T. P. Influence of Charge Fraction on the Phase Behavior of Symmetric Single-Ion Conducting Diblock Copolymers. *ACS Macro Lett.* **2021**, *10* (8), 1035–1040. <https://doi.org/10.1021/acsmacrolett.1c00393>.



- (30) Lozinskaya, E. I.; Ponkratov, D. O.; Shaplov, A. S.; Malyshkina, I. A.; Streltsov, D. R.; Bakirov, A. V. Methacrylate Single-Ion Conducting Block Copolymers: Effect of the Chemical Structure on Conductivity and Morphological Organization. *Polym. Sci. Ser. A* **2023**, *65* (1), 36–52. <https://doi.org/10.1134/S0965545X2370075X>.
- (31) Wen, K.; Xin, C.; Guan, S.; Wu, X.; He, S.; Xue, C.; Liu, S.; Shen, Y.; Li, L.; Nan, C.-W. Ion–Dipole Interaction Regulation Enables High-Performance Single-Ion Polymer Conductors for Solid-State Batteries. *Adv. Mater.* **2022**, *34* (32), 2202143. <https://doi.org/10.1002/adma.202202143>.
- (32) Guzmán-González, G.; Vauthier, S.; Alvarez-Tirado, M.; Cotte, S.; Castro, L.; Guéguen, A.; Casado, N.; Mecerreyes, D. Single-Ion Lithium Conducting Polymers with High Ionic Conductivity Based on Borate Pendant Groups. *Angew. Chem.* **2022**, *134* (7), e202114024. <https://doi.org/10.1002/ange.202114024>.
- (33) Liang, H.-P.; Zarrabeitia, M.; Chen, Z.; Jovanovic, S.; Merz, S.; Granwehr, J.; Passerini, S.; Bresser, D. Polysiloxane-Based Single-Ion Conducting Polymer Blend Electrolyte Comprising Small-Molecule Organic Carbonates for High-Energy and High-Power Lithium-Metal Batteries. *Adv. Energy Mater.* **2022**, *12* (16), 2200013. <https://doi.org/10.1002/aenm.202200013>.
- (34) Hatakeyama-Sato, K.; Kimura, S.; Matsumoto, S.; Oyaizu, K. Facile Synthesis of Poly(Glycidyl Ether)s with Ionic Pendant Groups by Thiol-Ene Reactions. *Macromol. Rapid Commun.* **2020**, *41* (1), 1900399. <https://doi.org/10.1002/marc.201900399>.
- (35) Dreier, P.; Pipertzis, A.; Spyridakou, M.; Mathes, R.; Floudas, G.; Frey, H. Introduction of Trifluoromethanesulfonamide Groups in Poly(Ethylene Oxide): Ionic Conductivity of Single-Ion-Conducting Block Copolymer Electrolytes. *Macromolecules* **2022**, *55* (4), 1342–1353. <https://doi.org/10.1021/acs.macromol.1c02507>.
- (36) Lee, J.; Kim, S.; Kwon, H.; Jo, S.; Ryu, D. Y.; Choi, U. H.; Kim, B.-S. Single-Ion-Conducting Polyether Electrolytes via Orthogonal Postpolymerization Modification. *Macromolecules* **2023**, *56* (18), 7520–7531. <https://doi.org/10.1021/acs.macromol.3c00985>.
- (37) Jing, X.; Hu, Z.; Qin, J.; Jiang, X.; Wang, M.; Huo, S.; Zhang, S.; Wang, J.; Zhang, Y. Highly Conductive and Mechanically Robust Single-Ion Conducting Polymer Electrolyte Membranes with a High Concentration of Charge Carriers for Dendrite-Proof Lithium Metal Batteries. *J. Membr. Sci.* **2023**, *688*, 122118. <https://doi.org/10.1016/j.memsci.2023.122118>.
- (38) Hu, Z.; Jing, X.; Chen, M.; Xu, H.; Zhang, Y.; Cheng, H. Multifunctional Single-Ion Conductor-Integrated PEO-Based Solid Polymer Electrolytes Endow Highly Stable and Dendrite-Free Lithium Metal Batteries. *Mater.* **2024**, *2*, 100090. <https://doi.org/10.1016/j.nxmate.2023.100090>.
- (39) Jagadesan, P.; Cui, J.; Kalami, S.; Abrha, L. H.; Lee, H.; Khani, H. Perfluorinated Single-Ion Li<sup>+</sup> Conducting Polymer Electrolyte for Lithium-Metal Batteries. *J. Electrochem. Soc.* **2024**, *171* (4), 040537. <https://doi.org/10.1149/1945-7111/ad3f51>.
- (40) Dong, X.; Chen, Z.; Gao, X.; Mayer, A.; Liang, H.-P.; Passerini, S.; Bresser, D. Stepwise Optimization of Single-Ion Conducting Polymer Electrolytes for High-Performance Lithium-Metal Batteries. *J. Energy Chem.* **2023**, *80*, 174–181. <https://doi.org/10.1016/j.jechem.2023.01.044>.
- (41) Shi, J.; Nguyen, H.-D.; Chen, Z.; Wang, R.; Steinle, D.; Barnsley, L.; Li, J.; Frielinghaus, H.; Bresser, D.; Iojoiu, C.; Paillard, E. Nanostructured Block Copolymer Single-Ion Conductors for Low-Temperature, High-Voltage and Fast Charging Lithium-Metal Batteries. *Energy Mater.* **2023**, *3* (4), N/A-N/A. <https://doi.org/10.20517/energymater.2023.27>.



- (42) Li, Z.; You, Y.; Liang, X.; Wang, P.; Zhang, Z.; Du, X.; Liu, B.; Sun, Z.; Hu, W. A Single Ion Polymer Electrolyte via Copolymerization of Lithium (4-Styrenesulfonyl)(Trifluoromethanesulfonyl)Imide and Allyl Poly(Aryl Ether Ketone) Enables Safe Lithium Ion Batteries. *Appl. Surf. Sci.* **2023**, *611*, 155363. <https://doi.org/10.1016/j.apsusc.2022.155363>. View Article Online  
DOI: 10.1039/C6TA01035K
- (43) Jones, S. D.; Nguyen, H.; Richardson, P. M.; Chen, Y.-Q.; Wyckoff, K. E.; Hawker, C. J.; Clément, R. J.; Fredrickson, G. H.; Segalman, R. A. Design of Polymeric Zwitterionic Solid Electrolytes with Superionic Lithium Transport. *ACS Cent. Sci.* **2022**, *8* (2), 169–175. <https://doi.org/10.1021/acscentsci.1c01260>.
- (44) Xu, H.; Huang, L.; Li, W.; Gu, S.; Zeng, D.; Zhang, Y.; Sun, Y.; Cheng, H. Shielding the Electrostatic Attraction by Design of Zwitterionic Single Ion Conducting Polymer Electrolyte with High Dielectric Constant. *J. Membr. Sci.* **2022**, *651*, 120452. <https://doi.org/10.1016/j.memsci.2022.120452>.
- (45) Du, D.; Li, H.; Xu, H.; Zhang, Y.; Sun, Y.; Zeng, D.; Cheng, H. Lithium Propanesulfonyl(Trifluoromethylsulfonyl)Imide Grafted Polybenzimidazole as a Self-Supporting Single Ion Conducting Polymer Electrolyte Membrane for Lithium Metal Secondary Batteries. *J. Alloys Compd.* **2021**, *881*, 160573. <https://doi.org/10.1016/j.jallcom.2021.160573>.
- (46) Xu, H.; Li, W.; Huang, L.; Zeng, D.; Zhang, Y.; Sun, Y.; Cheng, H. Zwitterion-Doped Self-Supporting Single-Ion Conducting Polymer Electrolyte Membrane for Dendrite-Free Lithium Metal Secondary Batteries. *Sci. CHINA Mater.* **2023**, *66* (10), 3799–3809. <https://doi.org/10.1007/s40843-023-2547-y>.
- (47) Zhang, W.; Feng, S.; Huang, M.; Qiao, B.; Shigenobu, K.; Giordano, L.; Lopez, J.; Tatara, R.; Ueno, K.; Dokko, K.; Watanabe, M.; Shao-Horn, Y.; Johnson, J. A. Molecularly Tunable Polyanions for Single-Ion Conductors and Poly(Solvate Ionic Liquids). *Chem. Mater.* **2021**, *33* (2), 524–534. <https://doi.org/10.1021/acs.chemmater.0c03258>.
- (48) Nguyen, N.; Blatt, M. P.; Kim, K.; Hallinan, D. T.; Kennemur, J. G. Investigating Miscibility and Lithium Ion Transport in Blends of Poly(Ethylene Oxide) with a Polyanion Containing Precisely-Spaced Delocalized Charges. *Polym. Chem.* **2022**, *13* (29), 4309–4323. <https://doi.org/10.1039/D2PY00605G>.
- (49) Paren, B. A.; Nguyen, N.; Ballance, V.; Hallinan, D. T.; Kennemur, J. G.; Winey, K. I. Superionic Li-Ion Transport in a Single-Ion Conducting Polymer Blend Electrolyte. *Macromolecules* **2022**, *55* (11), 4692–4702. <https://doi.org/10.1021/acs.macromol.2c00459>.
- (50) Park, J.; Staiger, A.; Mecking, S.; Winey, K. I. Enhanced Li-Ion Transport through Selectively Solvated Ionic Layers of Single-Ion Conducting Multiblock Copolymers. *ACS Macro Lett.* **2022**, *11* (8), 1008–1013. <https://doi.org/10.1021/acsmacrolett.2c00288>.
- (51) Fraile-Insagurbe, D.; Boaretto, N.; Aldalur, I.; Raposo, I.; Bonilla, F. J.; Armand, M.; Martínez-Ibañez, M. Novel Single-Ion Conducting Polymer Electrolytes with High Toughness and High Resistance against Lithium Dendrites. *Nano Res.* **2023**, *16* (6), 8457–8468. <https://doi.org/10.1007/s12274-023-5378-z>.
- (52) Wang, N.; Chen, X.; Sun, Q.; Song, Y. Single-Ion Conducting Polymer Electrolytes Based on Random Polyurethane–Urea with Different Diisocyanate Structures for Lithium Batteries. *ACS Appl. Energy Mater.* **2022**, *5* (4), 4743–4754. <https://doi.org/10.1021/acsaem.2c00149>.
- (53) Wang, N.; Qin, D.; Sun, Q.; Chen, X.; Song, Y.; Xin, T. Single-Ion Conducting Polyurethane-Ester Solid Polymer Electrolyte Membrane toward Lithium Metal Batteries. *ACS Appl. Polym. Mater.* **2023**, *5* (4), 2607–2616. <https://doi.org/10.1021/acsapm.2c02197>.



- (54) Wang, N.; Chen, X.; Sun, Q.; Song, Y.; Xin, T. Fast Li<sup>+</sup> Transport Polyurethane-Based Single-Ion Conducting Polymer Electrolyte with Sulfonamide Side Chains in the Hard Segment for Lithium Metal Batteries. *ACS Appl. Mater. Interfaces* **2023**, *15* (33), 39837–39846. <https://doi.org/10.1021/acsami.3c06956>. View Article Online  
DOI: 10.1039/D6TA01035K
- (55) Bocharova, V.; Chen, X. C.; Jeong, S. P.; Zhou, Z.; Sacci, R. L.; Keum, J. K.; Gainaru, C.; Rahman, M. A.; Sahori, R.; Sun, X.-G.; Cao, P.; Westover, A. Single Ion Conducting Hairy Nanoparticle Additive to Improve Cycling Stability of Solid Polymer Electrolytes. *ACS Appl. Energy Mater.* **2023**, *6* (15), 8042–8052. <https://doi.org/10.1021/acsaem.3c01106>.
- (56) Pantazidis, C.; Andreou, S.; Nikolakakou, G.; Glynos, E.; Sakellariou, G. Synthesis and Molecular Characterization of Well-Defined Polyanion Miktoarm Star Copolymers. *Polym. Chem.* **2022**, *13* (14), 1997–2007. <https://doi.org/10.1039/D2PY00195K>.
- (57) Cao, P.-F.; Wojnarowska, Z.; Hong, T.; Carroll, B.; Li, B.; Feng, H.; Parsons, L.; Wang, W.; Lokitz, B. S.; Cheng, S.; Bocharova, V.; Sokolov, A. P.; Saito, T. A Star-Shaped Single Lithium-Ion Conducting Copolymer by Grafting a POSS Nanoparticle. *Polymer* **2017**, *124*, 117–127. <https://doi.org/10.1016/j.polymer.2017.07.052>.
- (58) Chen, S.; Li, Y.; Wang, Y.; Li, Z.; Peng, C.; Feng, Y.; Feng, W. Cross-Linked Single-Ion Solid Polymer Electrolytes with Alternately Distributed Lithium Sources and Ion-Conducting Segments for Lithium Metal Batteries. *Macromolecules* **2021**, *54* (19), 9135–9144. <https://doi.org/10.1021/acs.macromol.1c01102>.
- (59) Liang, H.-P.; Chen, Z.; Dong, X.; Zinkevich, T.; Indris, S.; Passerini, S.; Bresser, D. Photo-Cross-Linked Single-Ion Conducting Polymer Electrolyte for Lithium-Metal Batteries. *Macromol. Rapid Commun.* **2022**, *43* (12), 2100820. <https://doi.org/10.1002/marc.202100820>.
- (60) He, Y.; Wang, C.; Zou, P.; Lin, R.; Hu, E.; Xin, H. L. Anion-Tethered Single Lithium-Ion Conducting Polyelectrolytes through UV-Induced Free Radical Polymerization for Improved Morphological Stability of Lithium Metal Anodes. *Angew. Chem. Int. Ed.* **2023**, *62* (38), e202308309. <https://doi.org/10.1002/anie.202308309>.
- (61) Wang, X.; Huang, P.; Zhong, Y.; Zhang, S.; Fu, J.; Ding, Y.; Chen, L.; Chen, G.; Lv, F.; Yuan, S. 3D Crosslinked Semi-Interpenetrating Single-Ion Hybrid Electrolytes for Dendrite-Free and High-Voltage Lithium Metal Batteries. *Chem. Eng. J.* **2025**, *522*, 168099. <https://doi.org/10.1016/j.cej.2025.168099>.
- (62) Engler, A.; Park, H.; Liu, N.; Kohl, P. A. Dicarboxylate Acrylate Based Single-Ion Conducting Polymer Electrolytes for Lithium Batteries. *J. Power Sources* **2023**, *574*, 233145. <https://doi.org/10.1016/j.jpowsour.2023.233145>.
- (63) Porcarelli, L.; Sutton, P.; Bocharova, V.; Aguirresarobe, R. H.; Zhu, H.; Goujon, N.; Leiza, J. R.; Sokolov, A.; Forsyth, M.; Mecerreyes, D. Single-Ion Conducting Polymer Nanoparticles as Functional Fillers for Solid Electrolytes in Lithium Metal Batteries. *ACS Appl. Mater. Interfaces* **2021**, *13* (45), 54354–54362. <https://doi.org/10.1021/acsami.1c15771>.
- (64) Nikolakakou, G.; Pantazidis, C.; Sakellariou, G.; Glynos, E. Ion Conductivity–Shear Modulus Relationship of Single-Ion Solid Polymer Electrolytes Composed of Polyanionic Miktoarm Star Copolymers. *Macromolecules* **2022**, *55* (14), 6131–6139. <https://doi.org/10.1021/acs.macromol.2c00620>.
- (65) Cao, P.-F.; Li, B.; Yang, G.; Zhao, S.; Townsend, J.; Xing, K.; Qiang, Z.; Vogiatzis, K. D.; Sokolov, A. P.; Nanda, J.; Saito, T. Elastic Single-Ion Conducting Polymer Electrolytes: Toward a Versatile Approach for Intrinsically Stretchable Functional Polymers. *Macromolecules* **2020**, *53* (9), 3591–3601. <https://doi.org/10.1021/acs.macromol.9b02683>.



- (66) Cai, Y.; Liu, C.; Yu, Z.; Wu, H.; Wang, Y.; Ma, W.; Zhang, Q.; Jia, X. A Flexible and Highly Conductive Quasi-Solid Single-Ion Polymer Electrolyte for High Performance Li-Metal Batteries. *J. Power Sources* **2022**, *537*, 231478. <https://doi.org/10.1016/j.jpowsour.2022.231478>. View Article Online  
DOI: 10.1039/D3TA01035K
- (67) Lee, S.; Song, J.; Cho, J.; Son, J. G.; Kim, T. A. Thermally Reprocessable Self-Healing Single-Ion Conducting Polymer Electrolytes. *ACS Appl. Polym. Mater.* **2023**, *5* (9), 7433–7442. <https://doi.org/10.1021/acsapm.3c01319>.
- (68) Gan, H.; Zhang, Y.; Li, S.; Yu, L.; Wang, J.; Xue, Z. Self-Healing Single-Ion Conducting Polymer Electrolyte Formed via Supramolecular Networks for Lithium Metal Batteries. *ACS Appl. Energy Mater.* **2021**, *4* (1), 482–491. <https://doi.org/10.1021/acsaem.0c02384>.
- (69) Gallastegui, A.; Del Olmo, R.; Criado-Gonzalez, M.; Leiza, J. R.; Forsyth, M.; Mecerreyes, D. Printable Single-Ion Polymer Nanoparticle Electrolytes for Lithium Batteries. *Small Sci.* **2024**, *4* (3), 2300235. <https://doi.org/10.1002/smssc.202300235>.
- (70) Herranz Berzosa, A.; Gallastegui, A.; Lingua, G.; Mantione, D.; Villaluenga, I.; O'Dell, L.; Forsyth, M.; Mecerreyes, D. Lithium Single-Ion Copolymer Nanoparticle Design for Salt-Free Quasi-Solid-State Electrolytes. *ACS Appl. Polym. Mater.* **2025**, *7* (4), 2286–2296. <https://doi.org/10.1021/acsapm.4c03256>.
- (71) Nikolakakou, G.; Pantazidis, C.; Papadakis, V. M.; Kenanakis, G.; Loppinet, B.; Sakellariou, G.; Glynos, E. Nanostructured Single-Ion Polymer Blend Electrolytes Composed of Polyanionic Particles and Low Molecular Weight PEO. *ACS Macro Lett.* **2023**, *12* (12), 1665–1671. <https://doi.org/10.1021/acsmacrolett.3c00543>.
- (72) Nikolakakou, G.; Pantazidis, C.; Sakellariou, G.; Glynos, E. Thermal Properties and Ion Redistribution in Nanostructured Single-Ion Polymer Electrolyte Blends Composed of Polyanionic Miktoarm Stars. *ACS Macro Lett.* **2026**. <https://doi.org/10.1021/acsmacrolett.6c00077>.
- (73) Olmedo-Martínez, J. L.; Del Olmo, R.; Gallastegui, A.; Villaluenga, I.; Forsyth, M.; Müller, A. J.; Mecerreyes, D. All-Polymer Nanocomposite as Salt-Free Solid Electrolyte for Lithium Metal Batteries. *ACS Polym. Au* **2024**, *4* (1), 77–85. <https://doi.org/10.1021/acspolymersau.3c00035>.
- (74) Zhang, J.; Wang, S.; Han, D.; Xiao, M.; Sun, L.; Meng, Y. Lithium (4-Styrenesulfonyl) (Trifluoromethanesulfonyl) Imide Based Single-Ion Polymer Electrolyte with Superior Battery Performance. *Energy Storage Mater.* **2020**, *24*, 579–587. <https://doi.org/10.1016/j.ensm.2019.06.029>.
- (75) Cheng, H.; Yan, C.; Orenstein, R.; Dirican, M.; Wei, S.; Subjaleandee, N.; Zhang, X. Polyacrylonitrile Nanofiber-Reinforced Flexible Single-Ion Conducting Polymer Electrolyte for High-Performance, Room-Temperature All-Solid-State Li-Metal Batteries. *Adv. Fiber Mater.* **2022**, *4* (3), 532–546. <https://doi.org/10.1007/s42765-021-00128-1>.
- (76) Zhou, M.; Liu, R.; Jia, D.; Cui, Y.; Liu, Q.; Liu, S.; Wu, D. Ultrathin Yet Robust Single Lithium-Ion Conducting Quasi-Solid-State Polymer-Brush Electrolytes Enable Ultralong-Life and Dendrite-Free Lithium-Metal Batteries. *Adv. Mater.* **2021**, *33* (29), 2100943. <https://doi.org/10.1002/adma.202100943>.
- (77) Shen, C.; Zhao, Q.; Shan, N.; Jing, B. B.; Evans, C. M. Conductivity–Modulus–T<sub>g</sub> Relationships in Solvent-Free, Single Lithium Ion Conducting Network Electrolytes. *J. Polym. Sci.* **2020**, *58* (17), 2376–2388. <https://doi.org/10.1002/pol.20200302>.
- (78) Ng, M.-F.; Sun, Y.; Seh, Z. W. Machine Learning-Inspired Battery Material Innovation. *Energy Adv.* **2023**, *2* (4), 449–464. <https://doi.org/10.1039/D3YA00040K>.



- No primary research results, software or code have been included and no new data were generated or analysed as part of this review.

[View Article Online](#)

DOI: 10.1039/D6TA01035K

